Theory of Image Formation and Diffraction

CCEM Summer School on Electron Microscopy
at McMaster University
June 2 to June 7, 2019

Pierre Stadelmann
Chemin Rouge 15
CH-1805 Jongny
Switzerland

June 4, 2019

Introduction

The theory of **diffraction** and **image formation** in the electron microscope is based on **models**, **approximations** and **methods**. ery simplified diagram of diffraction and imaging in the electron microscope:

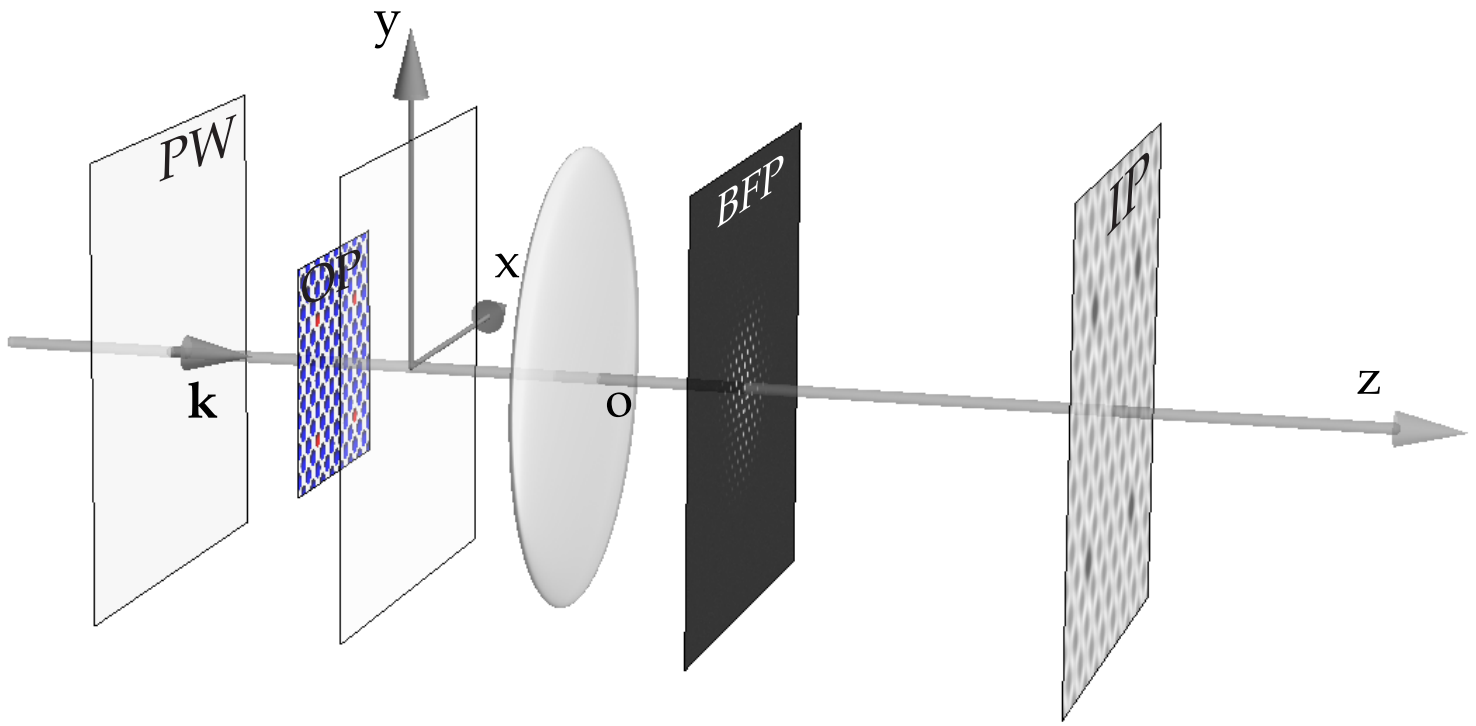

Simplified diagram of diffraction and imaging.

PW: Plane Wave (wave vector $\vec{k} \approx\!\!\parallel O_z$)
OP: Object Plane (where diffraction occurs)
BFP: Back Focal Plane (where transfer function of the microscope acts)
IP: Image Plane (detector plane)

Outline

: to describe diffraction and imaging we have to consider:

1. **Atomic scattering** → atomic scattering amplitude (atomic form factor).
2. **Object** → crystal or amorphous. For a crystal:
   - Lattice parameters → metric.
   - Symmetries → space-group, regular point system, Wyckoff positions.
   - Atoms position.
   - Orientation, ($[u, v, w]$ zone axis indices, (h, k, l) Laue circle center indices with u h + v k + w l = 0).
   - Shape (thickness, defect, ...).
3. **Diffraction**, i.e. scattering by object.
   - Single scattering event (kinematical diffraction).
   - Multiple scattering events (dynamical diffraction).
4. **Image formation** → Abbe theory.
5. **Microscope**
   - Source coherence (i.e. source size, energy spread).
   - Accelerating voltage.
   - Objective lens properties and aberrations
     (Cs: spherical aberration coefficient, Cc: chromatic aberration coefficient, ...).
   - HRTEM:partially coherent illumination (phase object + transfer function).
   - HRSTEM: incoherent illumination (optical transfer function).
6. **Detector** → image acquisition (modulation transfer function).

Approximations

Electron-matter interaction being very strong (10^4 X-Ray-matter) → **high energy electron**. To facilitate electron diffraction calculations these approximations are made:

1. **Atomic scattering amplitude**: Rutherford scattering, Born approximation.
2. **Small angle scattering** (i.e. accelerating voltage ≥ 50 kV).
3. **Relativistic electron mass** (Schrödinger equation).
4. **Elastic scattering** (energy conservation):
   - **Kinematical**: single scattering event.
   - **Dynamical**: multiple scattering events.
5. **Inelastic scattering**:
   - **Single** inelastic scattering.
   - **Multiple** inelastic scattering.
   - **Frozen** lattice or frozen phonon.
6. **Abbe imaging theory** either transmission cross-coefficients or transfer function + envelopes).

We make these approximations to describe TEM and STEM diffraction/imaging.

Methods

1. **Bloch wave** (solid state physics).
   Small unit cell crystals.

2. **Multislice** (physical optics).
   Large unit cell crystals.

3. **Abbe** imaging theory.
   Point Spread Function, Transmission Cross Coefficient.

One lens microscope...

The microscope is simplified and **only** the objective lens and axial aberrations considered, since it is the first imaging lens and its lateral magnification G_l is very large (HRTEM). Lateral magnification G_l corresponds to angular compression G_a since $G_l \times G_a = 1$.

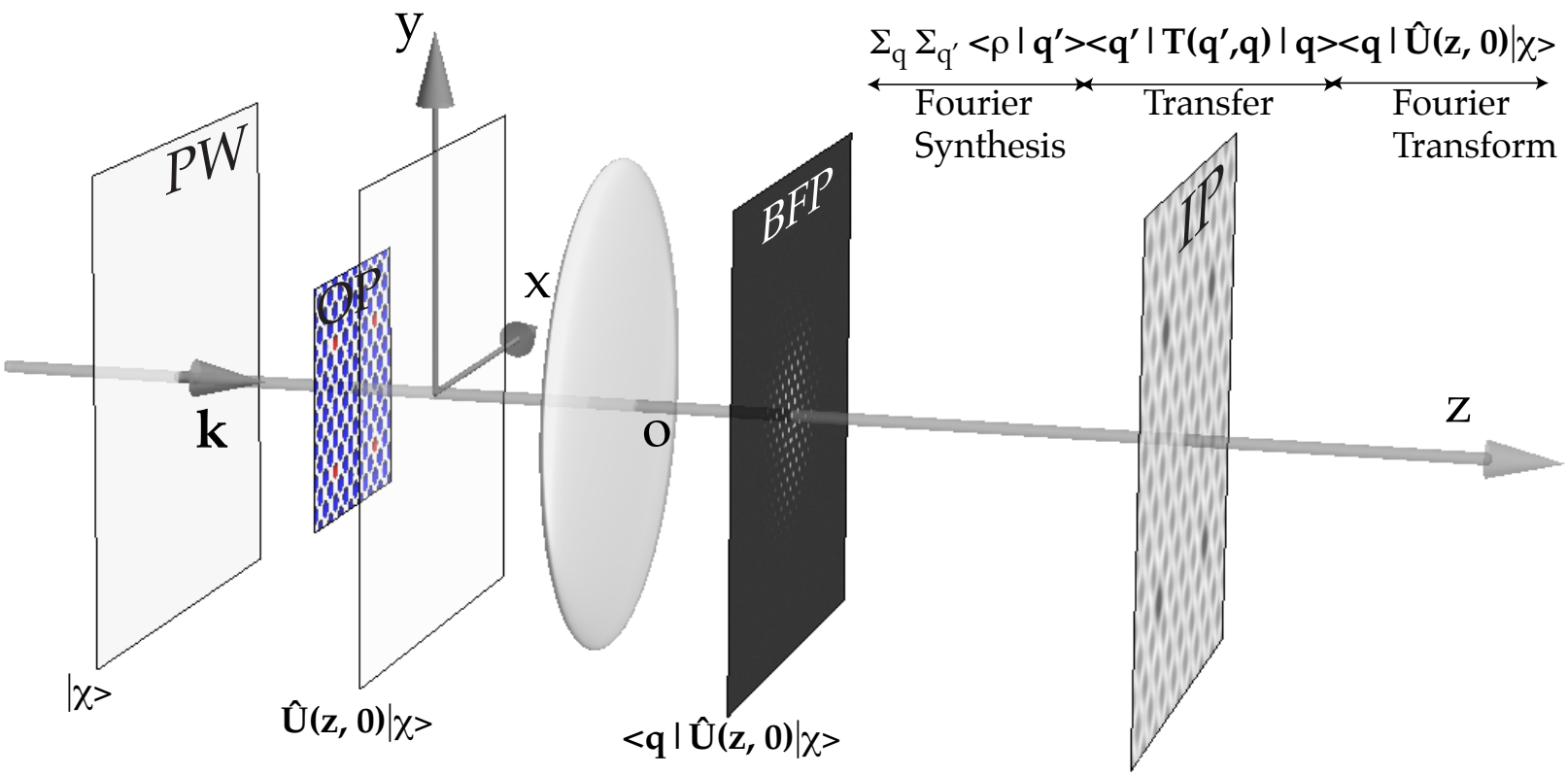

Diffraction and image formation: recommended books & articles

Recommended books are:

- J.M. Cowley, *Diffraction Physics*.
- P.B. Hirsch, A. Howie, R.B. Nicholson, W.D. Pashley & M.I. Whelan, *Electron Microscopy of Thin Crystals*.
- J.-P. Morniroli, *Large-Angle Convergent-Beam Electron Diffraction*.
- S.J. Pennycook & P.D. Nellist, *Scanning Transmission Electron Microscopy*.
- J.C.H. Spence, *High Resolution Electron Microscopy*.
- Z.L. Wang, *Elastic and Inelastic Electron Scattering in Electron Diffraction and Imaging*.
- E.J. Kirkland, *Advanced Computing in Electron Microscope*.

Recommended articles:

- J.M. Cowley & A.F. Moodie, Acta Cryst. **10**, (1957) 609-619.
- D. Gratias & R. Portier, Acta Cryst. **A39** (1983) 576-584.
- K. Ishizuka, Ultramicroscopy **5** (1980) 55-65, Ultramiscoscopy **90** (2002) 71-83.
- D. Van Dyck, Phys. Status Solidi **72** (1975) 321-336.

Scattering

Rutherford scattering: HAADF STEM imaging

For central potential, $V(r)$, **scattering angle** θ determined by **impact parameter** b.

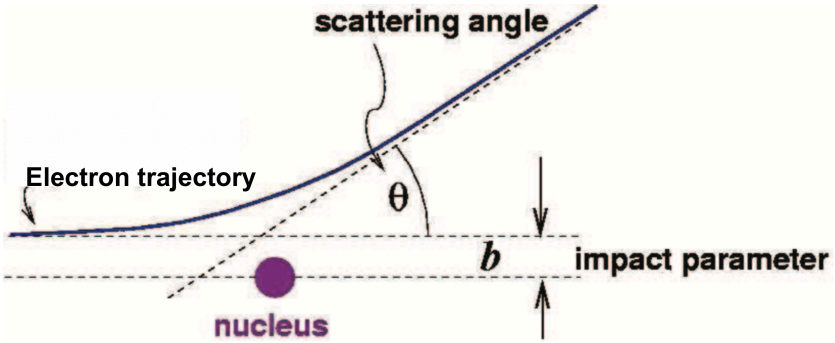

Number of particles N scattered per **unit time** between θ and $\theta + d\theta$ is equal to the number incident particles per (unit time) between b **and** $b + db$. For **incident flux** J_I, the number of particles N scattered into the **solid angle** $d\Omega = 2\pi sin\theta\, d\theta$ (per unit time):

$$N\, d\Omega = N\, 2\pi sin\theta\, d\theta = 2\pi b\, db\, J_I$$

$$\frac{d\sigma}{d\Omega} = \frac{b}{sin\theta}\left|\frac{db}{d\theta}\right|$$

Coulomb scattering $V(r) \sim \frac{1}{r}$:

$$\frac{d\sigma}{d\Omega} = \frac{b}{sin\theta}\left|\frac{db}{d\theta}\right| \sim \frac{1}{sin^4\left(\frac{\theta}{2}\right)}$$

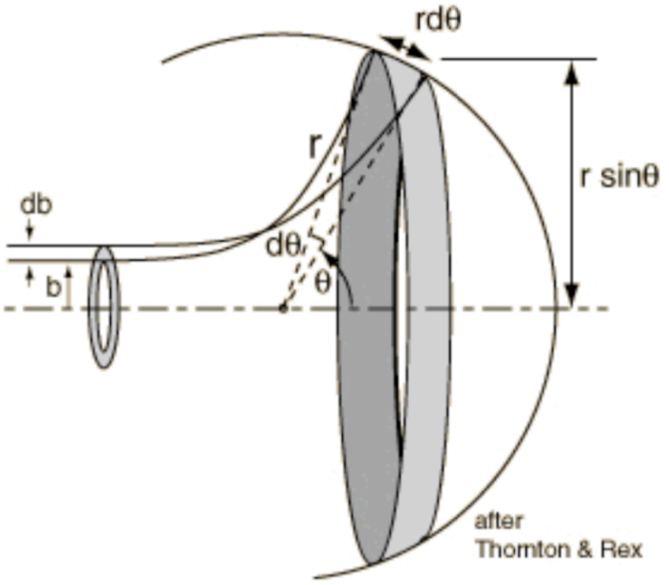

Quantum scattering

Simplest scattering experiment: plane wave impinging on localised potential, $V(r)$, e.g. electron striking atom.

Assumption: constant flux of **mono-kinetic** electrons, scattered from target and collected by detectors which measure angles of deflection.

In principle, if all incoming particles are represented by wave-packets, one has to solve **time-dependent Schrödinger equation**:

$$i\hbar\partial_t\Psi(\vec{r},t) = \left[-\frac{\hbar^2}{2m}\Delta + V(\vec{r})\right]\Psi(\vec{r},t)$$

and find probability amplitudes for outgoing waves.

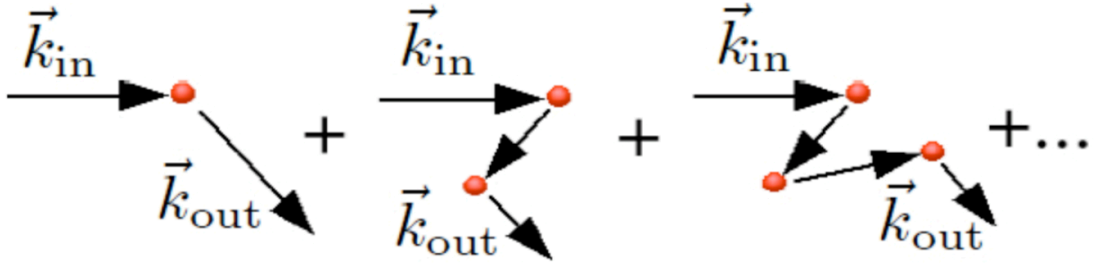

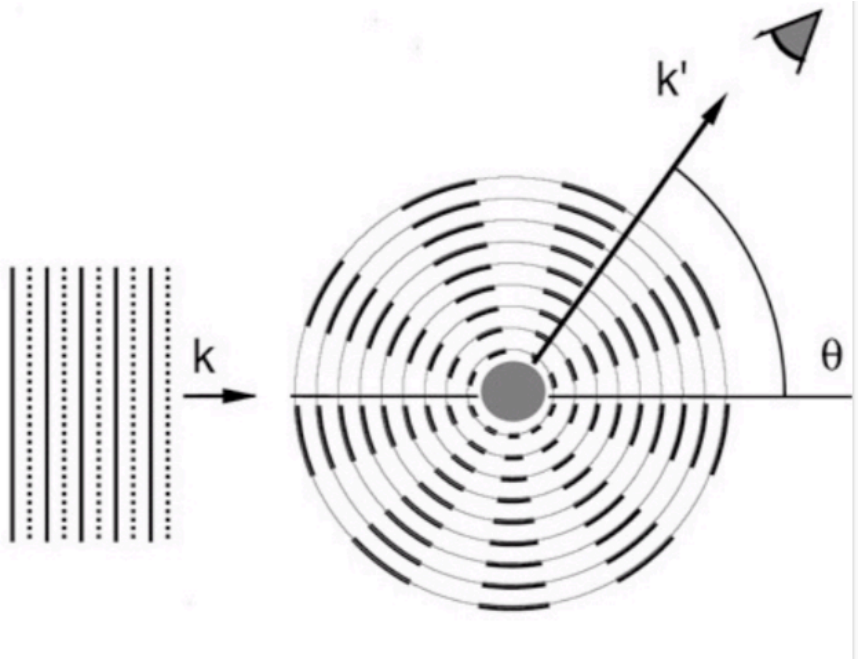

$$\Psi(\vec{r}) = e^{i\vec{k}\cdot\vec{r}} + f(\theta)\frac{e^{ikr}}{r}$$

Differential scattering cross section:

$$\frac{d\sigma}{d\Omega} = |f(\theta)|^2$$

X-Ray and electron scattering amplitude: atomic form factor

Atomic form factor: $f(\vec{\mathbf{q}}) = \int \rho(\vec{r}) e^{-i\vec{\mathbf{q}}\cdot\vec{r}} d^3\vec{r}$

$\vec{q}$: momentum transfer

Tabulation as a function of scattering vector: $s = \frac{\sin\theta}{\lambda}$

λ: wavelength

XRay diffraction

X-rays are scattered by the **electron cloud** of the atom (electron charge density $\rho_e(\vec{r})$)

$$f_x(s, Z) = \sum_{i=1}^{4} a_i \exp\left(-b_i(\frac{s}{4\pi})^2\right) + c$$

Electron diffraction

Electron are scattered by the **potential** distribution of the atom ($\rho(\vec{r})$)

$$f_e(s, Z) = \frac{me^2}{32\pi^3\hbar^2\epsilon_0}\left(\frac{Z - f_x(s, Z)}{s^2}\right)$$

Atomic scattering amplitudes

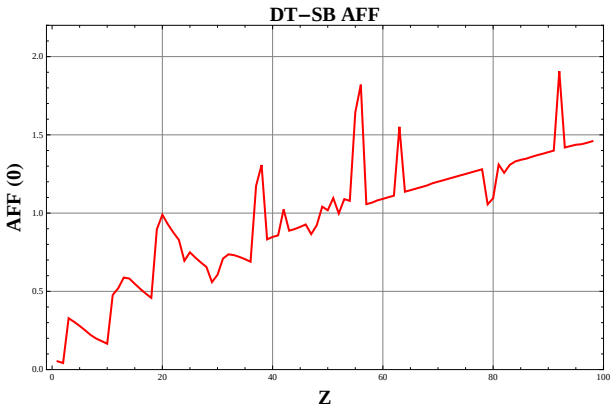

Doyle-Turner & Smith-Burge.

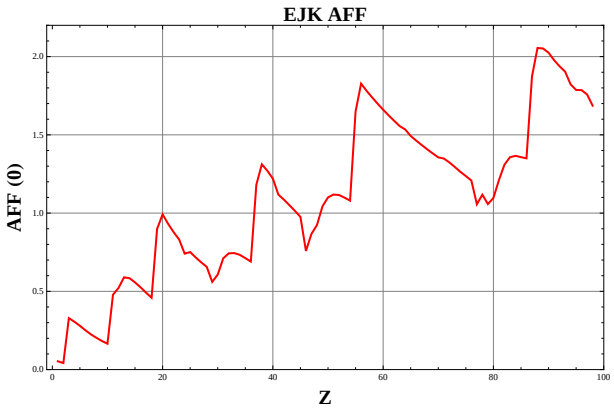

E.J. Kirkland.

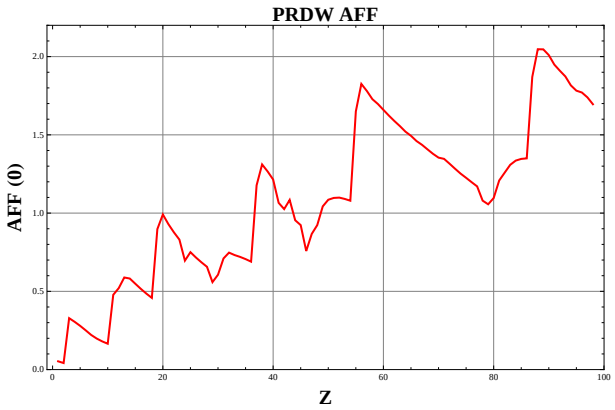

Peng-Ren-Dudarev-Whelan

$f_e(0)$ **from 3 tabulations of atomic scattering amplitudes.**

Weickenmaier - Kohl tabulation includes phonon and core loss absorption[1].

[1] A. Weickenmaier - H.Kohl, Computation of Absorptive Form Factors for High-Energy Electron Diffraction, Acta Cryst. (1991). A47, 590-597.

Scattering

The tabulated atomic scattering amplitudes are employed to calculate the object potential $V(\vec{r})$.

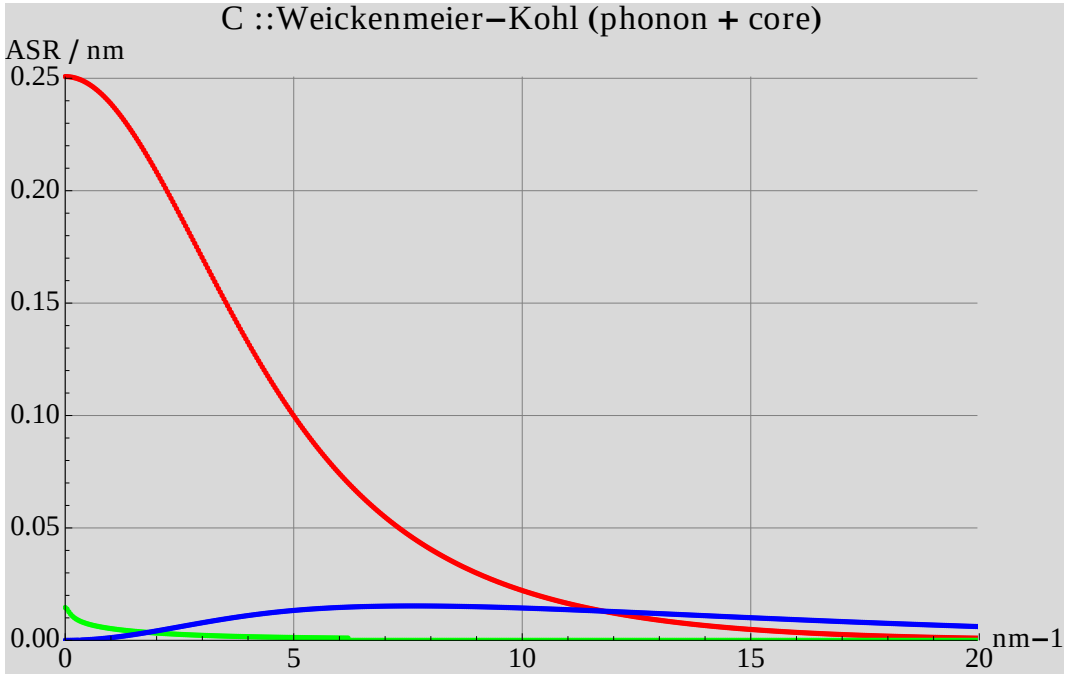

Atomic Scattering Amplitude (carbon), red: elastic, green: core absorption, blue: TDS (Thermal Diffuse Scattering).

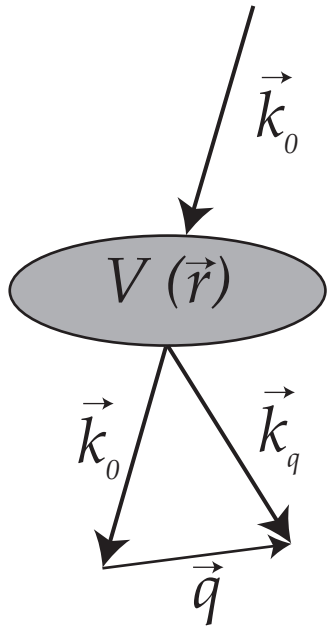

Electrons interact with the object potential $V(\vec{r})$.

Object

Object: Crystal

Object are not necessarily crystalline.

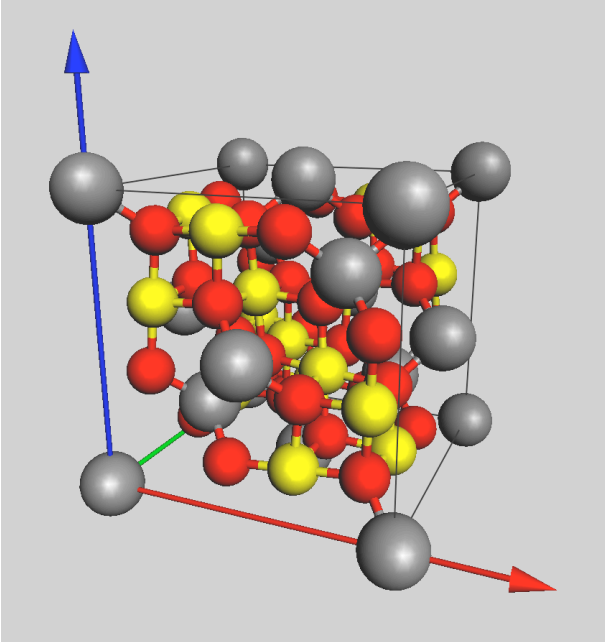

CoCr2O4
(cubic, F d -3 m, 3 atoms).

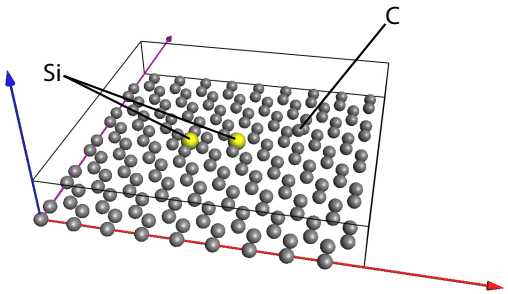

Graphene sheet
with add atoms (448 atoms).

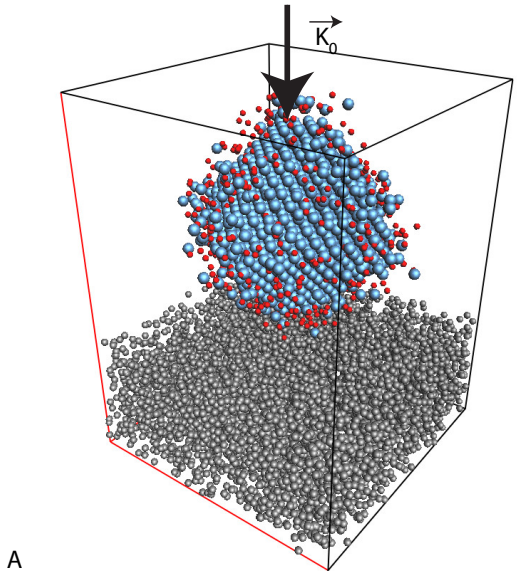

Pt catalyst
(Pt cube octahedron on amorphous carbon film, 10'000 atoms).

A **object** → **box** of parameters (a, b, c, α, β, γ) with atoms at (x, y, z) $(0.0 \leq (x, y, z) < 1.0)$.
The symmetries (space-group) help define the structure, the extinctions, etc.

Wrong models do not provide reliable HRTEM or HRSTEM simulated images!

Diffraction

Diffraction under kinematical approximation: single scattering by 10^n atoms

Diffraction = scattering by many scattering centers (atoms) and interference of spherical waves emitted by the centers.

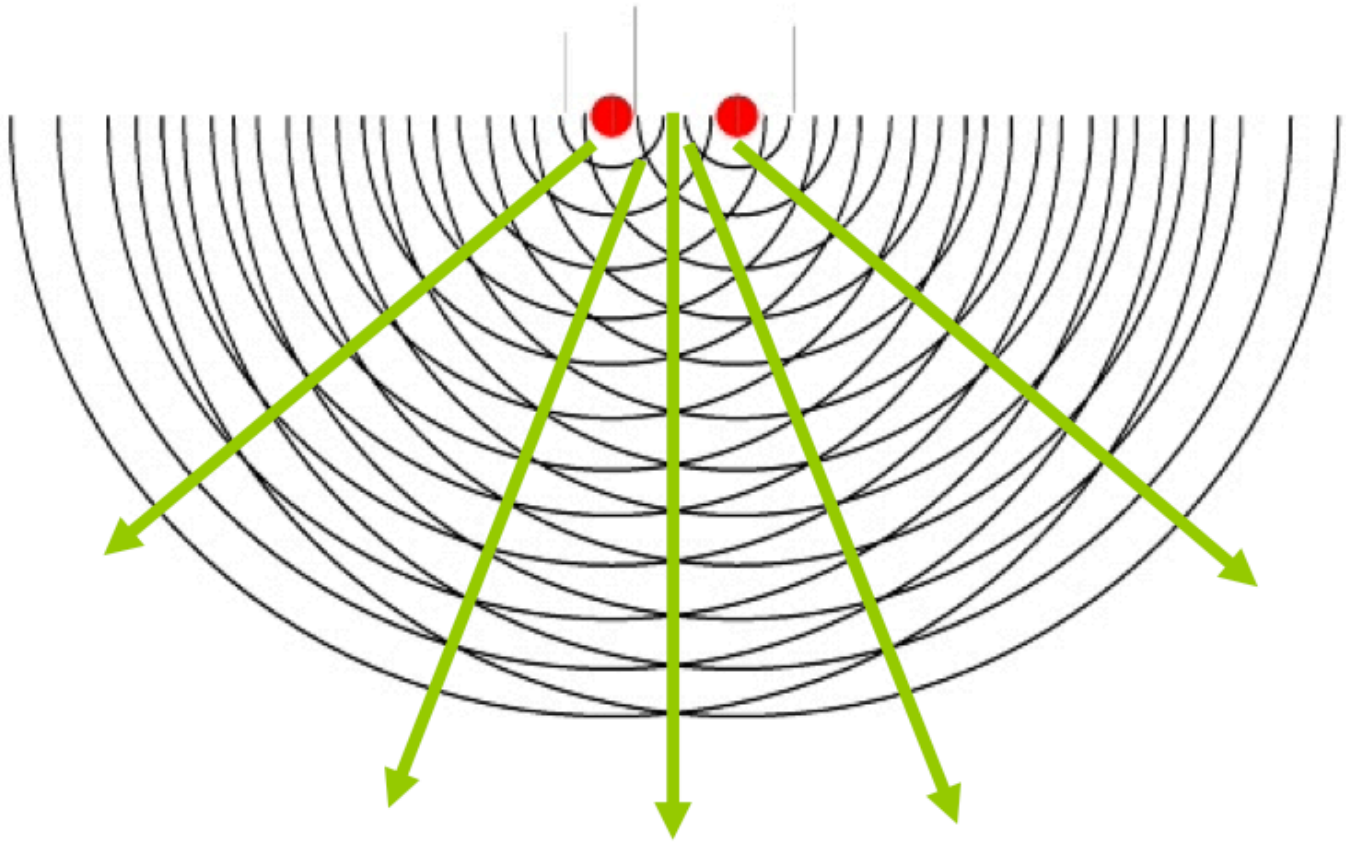

A crystal scatters the incident beam of electrons in directions given by the **Bragg** law. The larger the number of scattering centers the smaller the angular spread of the diffracted beams.

Diffraction: reciprocal space & Ewald sphere construction

- A sphere of radius $\frac{1}{\lambda}$ that intersects the origin of the reciprocal lattice.
- k_0 and k_s wave-vectors are radii.
- Diffraction occurs for any reciprocal lattice point on the Ewald sphere.
- In electron diffraction, the Ewald sphere condition is relaxed since the crystal is thin.

Bragg law (energy conservation):

$$|\vec{k_0} + \vec{G}| = |\vec{k_s}|$$

$$k_0^2 + 2 \times k_i \times G \times \cos(\vec{k_0}, \vec{G}) + G^2 = k_s^2$$

$$2k_0 \times \cos(\vec{k_i}, \vec{G}) = -G$$

$$2k_0 \times \cos(90^o - \theta_B) = -G$$

$$\frac{2}{\lambda} \times \sin(\theta_B) = G = \frac{1}{d_G}$$

$$2 \times d_{hkl} \times \sin(\theta_B) = \lambda$$

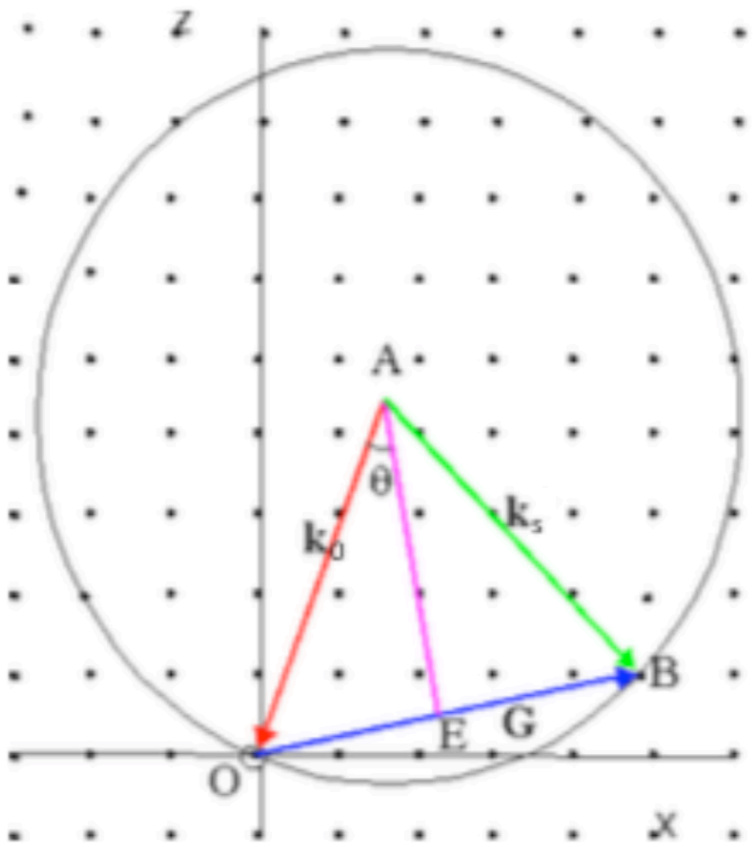

Metric of reciprocal space $g^* = g^{-1}$

$$g = \begin{bmatrix} a^2 & ab\cos\gamma & ac\cos\beta \\ ab\cos\gamma & b^2 & bc\cos\alpha \\ ac\cos\beta & bc\cos\alpha & c^2 \end{bmatrix}$$

Typical Bragg angles

At 100 kV, Bragg angles for several reflections of Al are given in the next table.

(hkl)	*Bragg angle* $[mrad]$	*Bragg angle* $[deg.]$	(hkl) *spacing* $[nm^{-1}]$
(1,1,1)	7.91	0.453	4.276
(2,0,0)	9.14	0.523	4.938
(2,2,0)	12.92	0.740	6.983
(1,1,3)	15.15	0.868	8.189
(2,2,2)	15.83	0.906	8.553
(4,0,0)	18.28	1.047	9.876

Bragg angles for some Al reflections at 100 kV.

Notice that the Bragg angles are pretty small (of the order a few ^{o}) and consequently the small angle approximation is quite good.

Intensity in the single scattering approximation: kinematic theory

Kinematically the intensity of any (hkl) reflection (or diffracted spot as observed on a CCD camera) is proportional to I_{hkl}:

$$I_{hkl} \sim F^*_{hkl} F_{hkl}$$

where the structure factor F_{hkl} is:

$$F_{hkl} = \sum_{i=atoms} f_i(s_{hkl}) \exp^{-[2\imath\pi(h x_i + k y_i + l z_i)]} occ_i \, DW_i(hkl)$$

Where for atom **i**:

- $f_i(s_{hkl})$: atomic scattering amplitude.
- x_i, y_i, z_i: (x,y,z) fractional coordinates ([0, 1[).
- occ_i: site occupancy.
- DW_i: Debye-Waller temperature factor.

Single scattering approximation is only valid for extremely thin crystals, but allows fast drawing of diffraction patterns.

Single scattering: kinematical diffraction plot

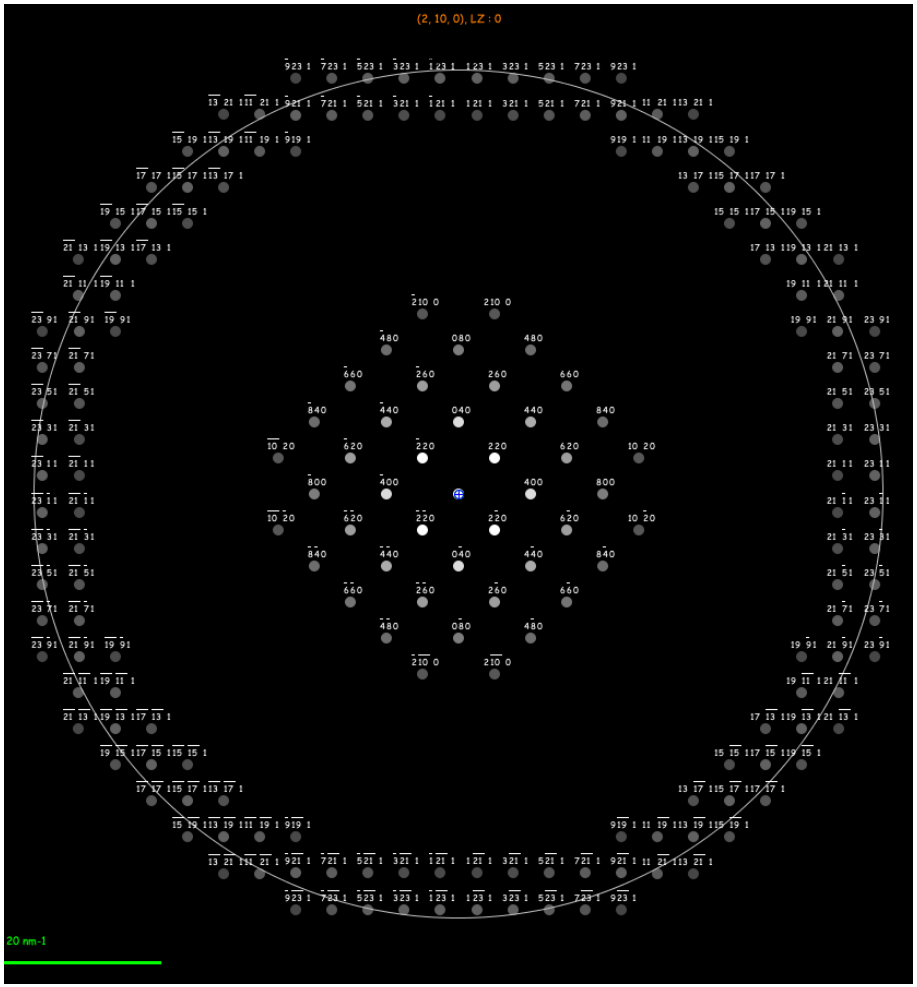

Si [001], ZOLZ and FOLZ reflections.

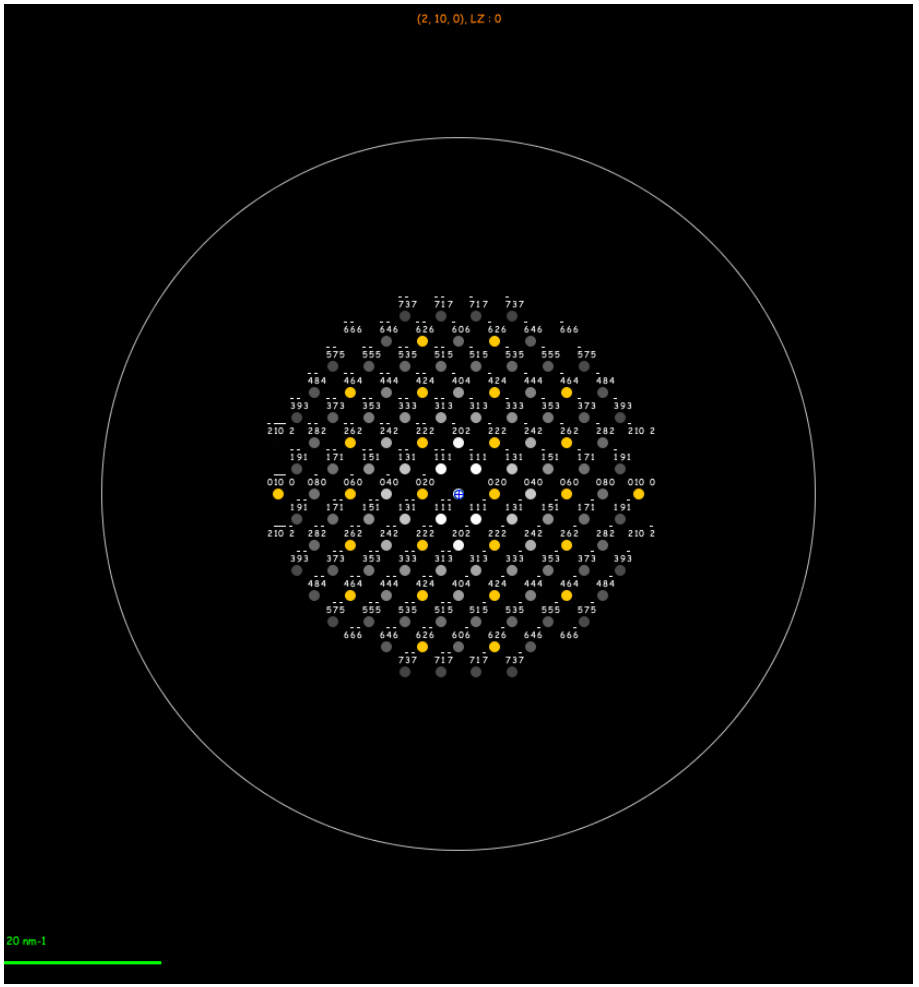

Si [110], ZOLZ reflections, the FOLZ reflections are missing (systematic extinctions in yellow).

Multiple scattering: diffraction geometry

Single scattering approximation is almost **never** realised in electron microscopy due to the very strong electron-matter interaction. Multiple scattering is the rule and is understood solving the **Schrödinger** equation for the proper diffraction geometry.

- Electron microscope favors O_z direction $\Longrightarrow$ i.e. destroys the space isotropy.
- 3-D space described a coordinate system $(\rho; z)$ where $\rho = \{x, y\}$ coordinates of on plane O_{xy} perpendicular to O_z.
- O_z anti-parallel to optical axis of electron microscope.
- Incident electron beam $\vec{K}_0$ anti-parallel to O_z axis and parallel optical axis.
- Crystal zone axis $\vec{u} = [u, v, w]$ parallel or nearly parallel to O_z.
- z-component of $\mathbf{K}_0$ (k_z) very large compared to χ.

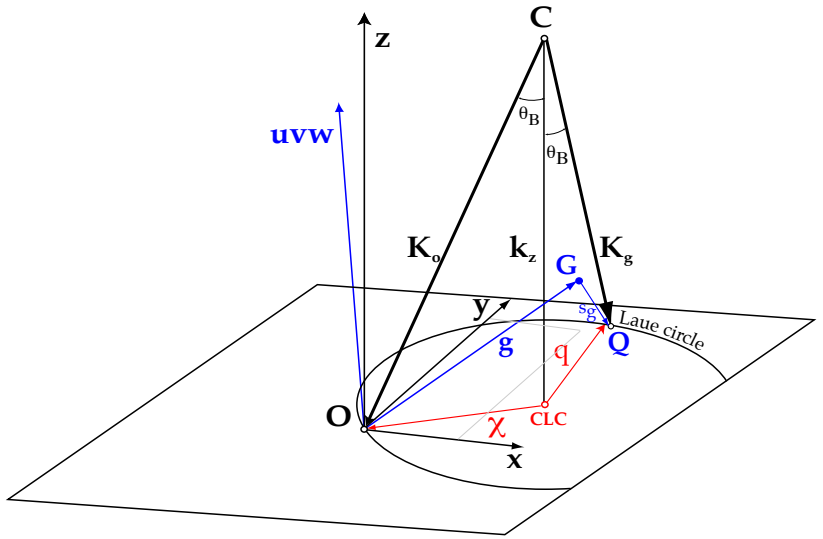

C: center of Ewald sphere

CLC: center of Laue circle

Electron wave oscillates with very high frequency in O_z direction: $e^{2\pi\imath k_z z}\Psi(\rho; z)$

Schrödinger equation

The Laplacian $\triangle = \frac{\partial^2}{\partial x^2} + \frac{\partial^2}{\partial y^2} + \frac{\partial^2}{\partial z^2}$ is written as: $\triangle_\rho + \frac{\partial^2}{\partial z^2}$. As a result, $[\triangle + ...]e^{2\pi\imath k_z z}\Psi(\rho;z)$ is given by: $[\triangle_\rho + \frac{\partial^2}{\partial z^2} + ...]e^{2\pi\imath k_z z}\Psi(\rho;z)$.
Performing the z-differentiation:

$$\frac{\partial^2}{\partial z^2}e^{2\pi\imath k_z z}\Psi(\rho;z) = e^{2\pi\imath k_z z}[-4\pi^2 k_z^2 + 4\pi\imath k_z\frac{\partial}{\partial z} + \frac{\partial^2}{\partial z^2}]\Psi(\rho;z)$$

Inserting the last expression and dropping the term $e^{2\pi\imath k_z z}$:

$$[\triangle_\rho + 4\pi^2(K_i^2 - k_z^2 + V(\rho;z)) + 4\pi\imath k_z\frac{\partial}{\partial z} + \frac{\partial^2}{\partial z^2}]\Psi(\rho;z) = 0$$

Since $K_i^2 = k_z^2 + \chi^2$:

$$[\triangle_\rho + 4\pi^2\chi^2 + 4\pi^2 V(\rho;z) + 4\pi\imath k_z\frac{\partial}{\partial z} + \frac{\partial^2}{\partial z^2}]\Psi(\rho;z) = 0$$

Rearranging the last equation:

$$\imath\frac{\partial\Psi(\rho;z)}{\partial z} = -\frac{1}{4\pi k_z}[\triangle_\rho + 4\pi^2\chi^2 + 4\pi^2 V(\rho;z) + \frac{\partial^2}{\partial z^2}]\Psi(\rho;z)$$

Fundamental equation

$$\imath\frac{\partial\Psi(\rho;z)}{\partial z}=-\frac{1}{4\pi k_z}[\triangle_\rho+4\pi^2\chi^2+4\pi^2V(\rho;z)+\frac{\partial^2}{\partial z^2}]\Psi(\rho;z)$$

The term $|\frac{\partial^2\Psi(\rho;z)}{\partial z^2}|$ being much smaller than $|k_z\frac{\partial\Psi(\rho;z)}{\partial z}|$ we drop it (this is equivalent to neglect backscattering).

Fundamental equation of elastic scattering of high energy mono-kinetic electrons with a potential within the approximation of small angle scattering:

$$\imath\frac{\partial}{\partial z}\Psi(\rho;z)=-\frac{1}{4\pi k_z}[\triangle_\rho+4\pi^2\chi^2+4\pi^2V(\rho;z)]\Psi(\rho;z)$$

Time dependent **Schrödinger** equation $\Longrightarrow$ solution by many methods of quantum mechanics!

Fundamental equation in Hamiltonian form:

$$\imath\frac{\partial}{\partial z}\Psi=\widehat{H}\ \psi$$

where:

$$\widehat{H}=-\frac{1}{4\pi k_z}[\triangle_\rho+4\pi^2\chi^2+4\pi^2V(\rho;z)]=H_o+\frac{4\pi^2V(\rho;z)}{4\pi k_z}$$

Remarks

- The approximations of the fundamental equation are equivalent to assume that the scattering potential is small compared to the accelerating potential and that k_z varies only slightly with z. It is in fact a quite good approximation, since the mean crystal potential is of the order of $10-30\ V$.
- Electron backscattering is neglected, the electrons are moving forwards.
- The fundamental equation is actually equivalent to a 2-dimensional **Schrödinger** equation ($\rho = \{x, y\}$) where z plays the role of time.

The system evolution is causal, from the past to the future:

$$\Psi(z) = \widehat{U}(z,0)\Psi(0)$$

A fundamental postulate of quantum mechanics says that the evolution operator obeys the equation:

$$\imath\frac{\partial}{\partial z}\widehat{U}(z,0) = \widehat{H}(\rho;z)\ \widehat{U}(z,0)$$

Causal evolution operator

$\widehat{U}(z,0)$: unitary operator (the norm of $|\Psi>$ is conserved), in general not directly integrable $\Longrightarrow$ approximations. The general solution is:

$$\widehat{U}(z,0) = e^{-\imath \int_0^z \widehat{H}(\tau)\, d\tau}$$

$\widehat{U}(z,0)$ can be directly integrated only when $\widehat{H}(\rho;z)$ and $\frac{\partial}{\partial z}\widehat{H}(\rho;z)$ commute:

$$\widehat{U}(z,0) = e^{-\imath \widehat{H} z}$$

$\widehat{H}(\rho;z)$ and $\frac{\partial}{\partial z}\widehat{H}(\rho;z)$ commute when:

- $V(\rho;z)$ does not depend on z, i.e. $V(\rho;z) = V(\rho)$(perfect crystal).
- $V(\rho;z)$ can be neglected (free space propagation).
- $\widehat{H}(\rho;z)$ is approximated by it potential term (phase object).

When $\widehat{H}$ depends on z, we can cut the object into thinner slices and use:

$$\Psi(z) = \widehat{U}(z,z_n)\widehat{U}(z_n,z_{n-1})...\widehat{U}(z_2,z_1)\widehat{U}(z_1,0)\Psi(0)$$

Intensity of diffracted beam $|q>$

The transition probability from initial state $|\chi>$ to final state $|q>$.

$$\omega_{\chi \rightarrow q}(z,0) = |<q|\widehat{U}(z,0)|\chi>|^2$$

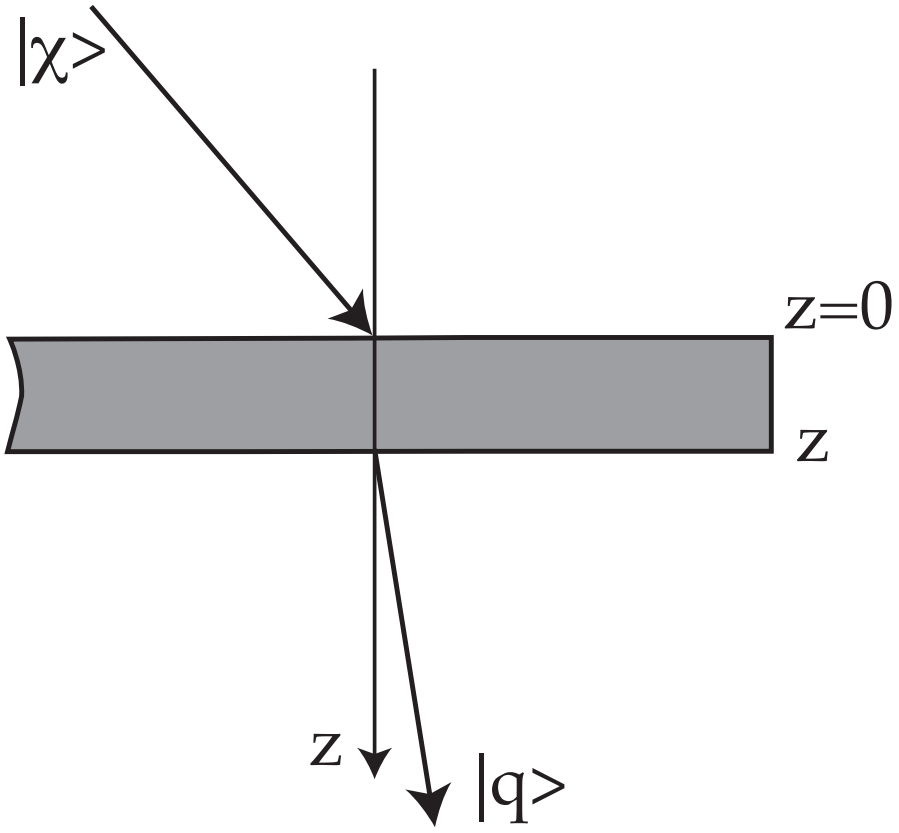

To calculate the intensity or transition probability $\omega_{\chi \rightarrow q}(z,0)$ we must calculate $\widehat{U}(z,0)$

Diffraction

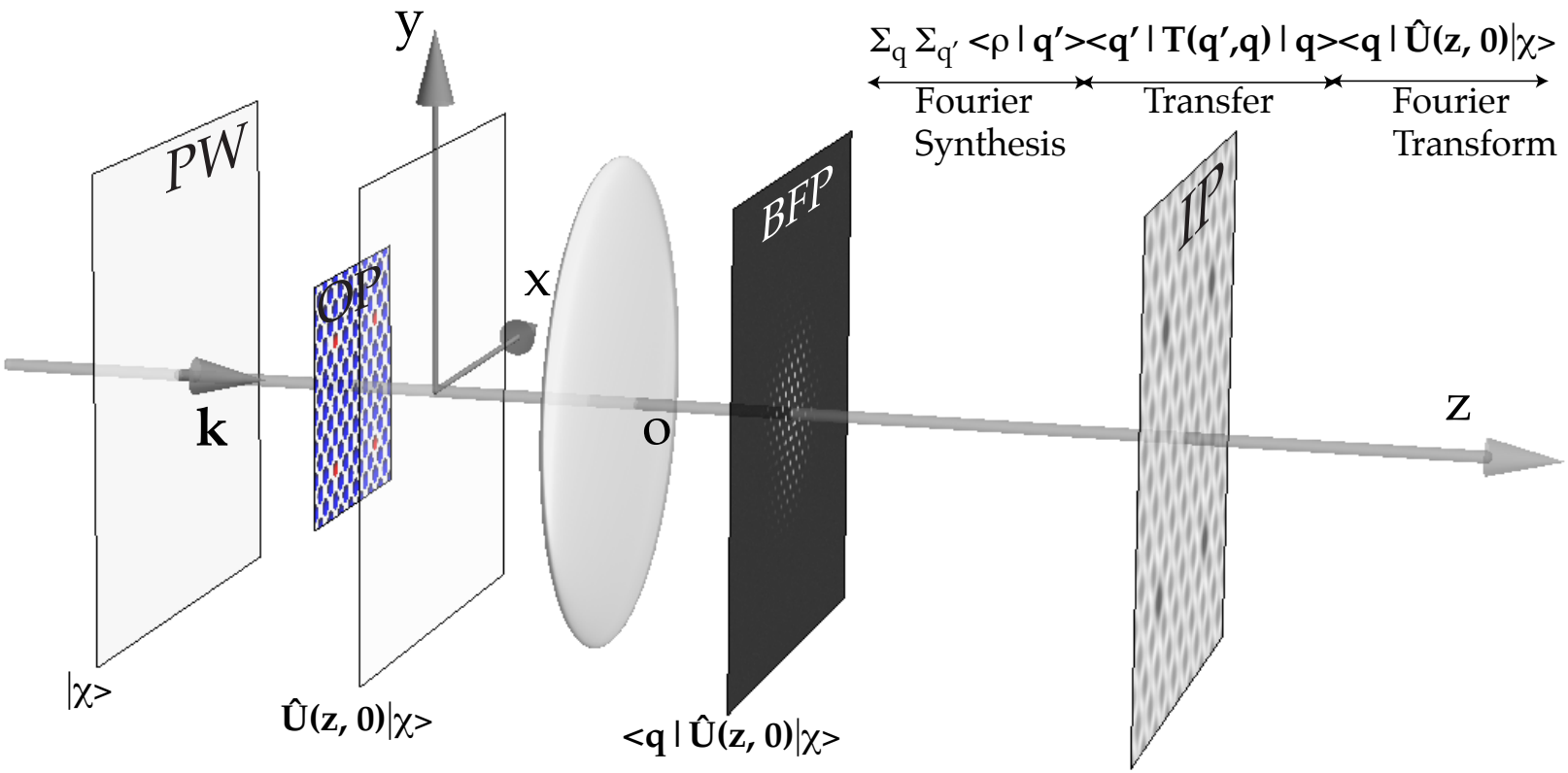

Methods to determine $\widehat{U}(z,0)$

$$H(z) = \frac{1}{2K}\left(-\nabla^2 - \chi^2 + V(z)\right) = H^0 + \frac{V(z)}{2K}$$

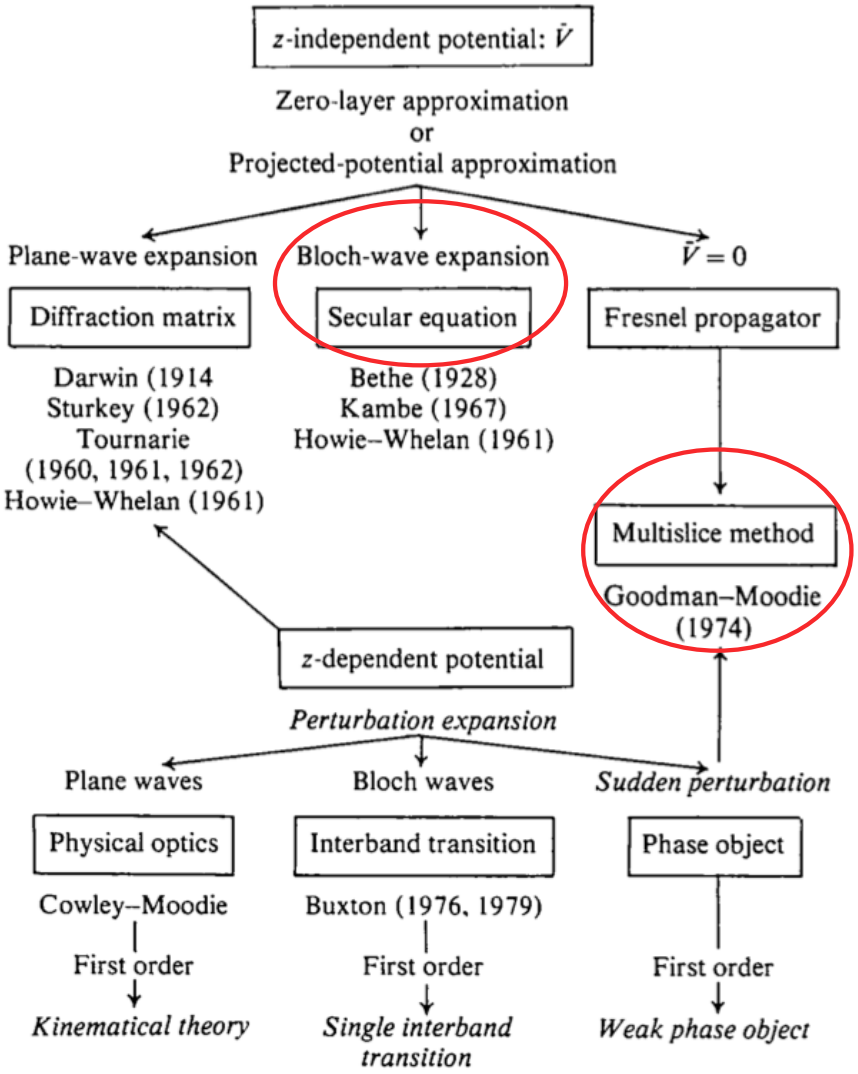

From Gratias and Portier[2].

[2] D. Gratias and R. Portier, Time-Like Perturbation Method in High-Energy Electron Diffraction, Acta Cryst. **A39** (1983) 576-584

Bloch wave method: z-independent potential

When the scattering potential is periodic, the eigenstates $|j>$ of the propagating electrons are Bloch waves. The hamiltonian of the system is projected on its eigenstates $|j>$ of eigenvalues γ_j (*"anpassung"* parameter).

$$\widehat{H} = \sum_j \gamma_j |j><j|$$

The evolution operator is then given by (since $V = V(\vec{\rho})$):

$$\widehat{U}(z,0) = e^{-i\widehat{H}z} = \sum_j e^{-i\gamma_j z}|j><j|$$

The wave-function at z developed on plane waves basis $|q>$:

$$\Psi(z) = \sum_q \phi_q(z)|q>$$

$$\phi_q(z) = <q|\widehat{U}(z,0)|0> = \sum_j e^{-i\gamma_j z} <q|j><j|0>$$

$$c_0^{*j} = <j|0> \text{ and } c_q^j = <q|j>$$

where in usual notation c_0^{*j} and c_q^j are the Bloch-wave excitations (component of the initial state $|0>$ on $|j>$) and coefficients (component of reflection $|q>$ on $|j>$) respectively[3].

[3] C. Humphreys & R.M. Fisher, Bloch Wave Notation in Many-Beam Electron Diffration, Acta Cryst. **A27** (1971) 42-45.

Bloch wave versus multislice

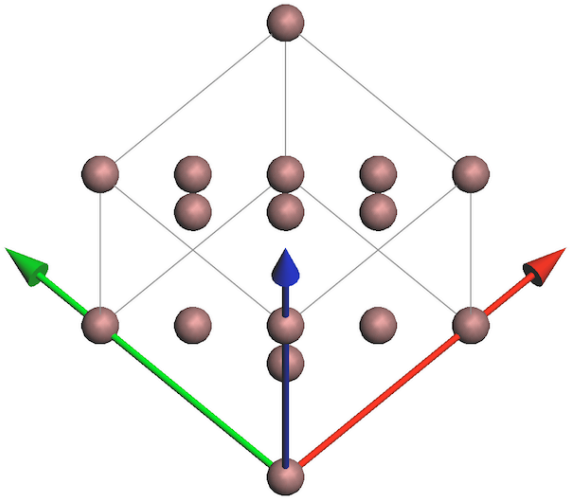

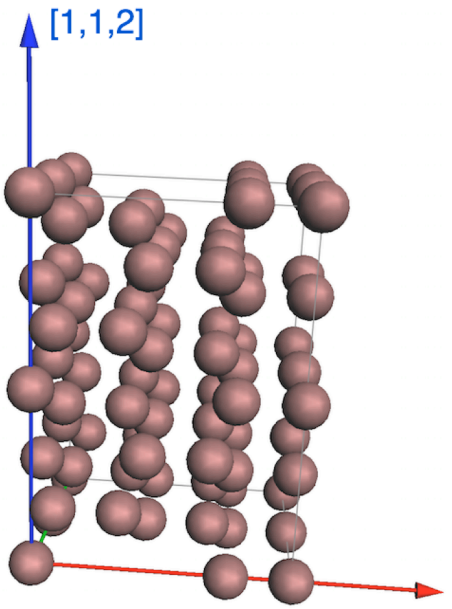

Si unit cell for [112] **Bloch wave** simulations (1 unit cell, 8 atoms).

Si unit cell for [112] **multislice** simulations (6 x Si unit cells, 48 = 6 x 8 atoms).

When using the multislice method, slicing the unit cell in general [uvw] directions may be pretty complicated. On the contrary using the Bloch wave method slicing is not necessary and High Order Laue Zones (HOLZ) reflections straightforward to include, since reflections are directly introduced in the simulations.

Dynamical scattering: Si [110]

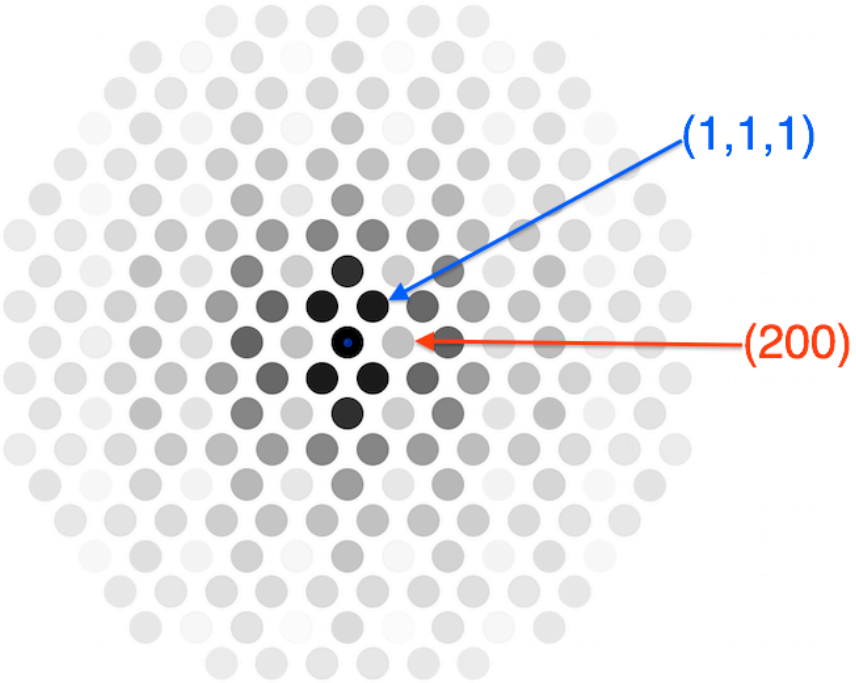

2 unit cell thick Si [110].

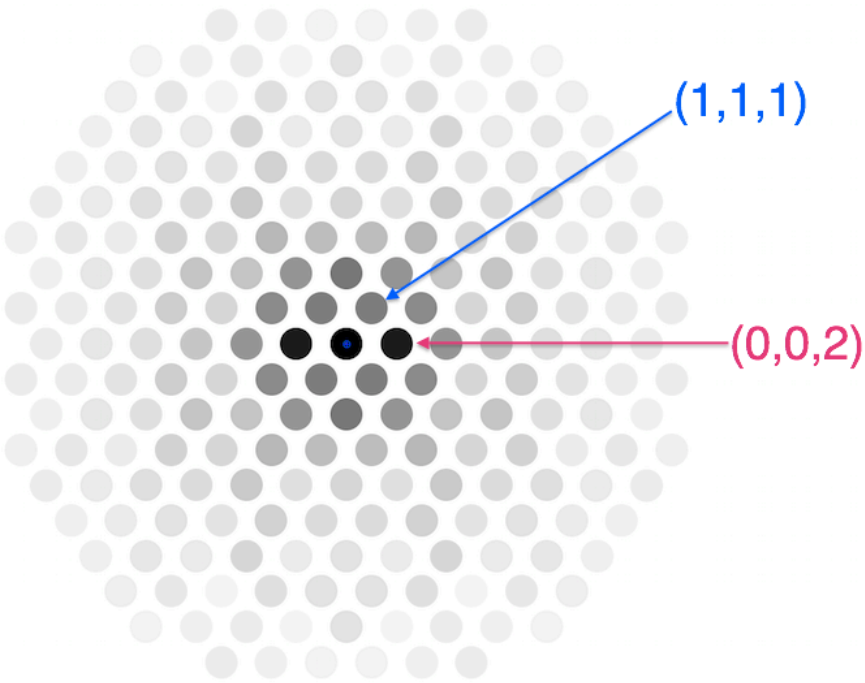

50 unit cells thick Si [110].

Very often for particular crystal thicknesses forbidden reflections are more intense than regular reflections. Example Si [110] where $I_{(002)} > I_{(111)}$.

Dynamical scattering: $CoCr_2O_4$ [001]

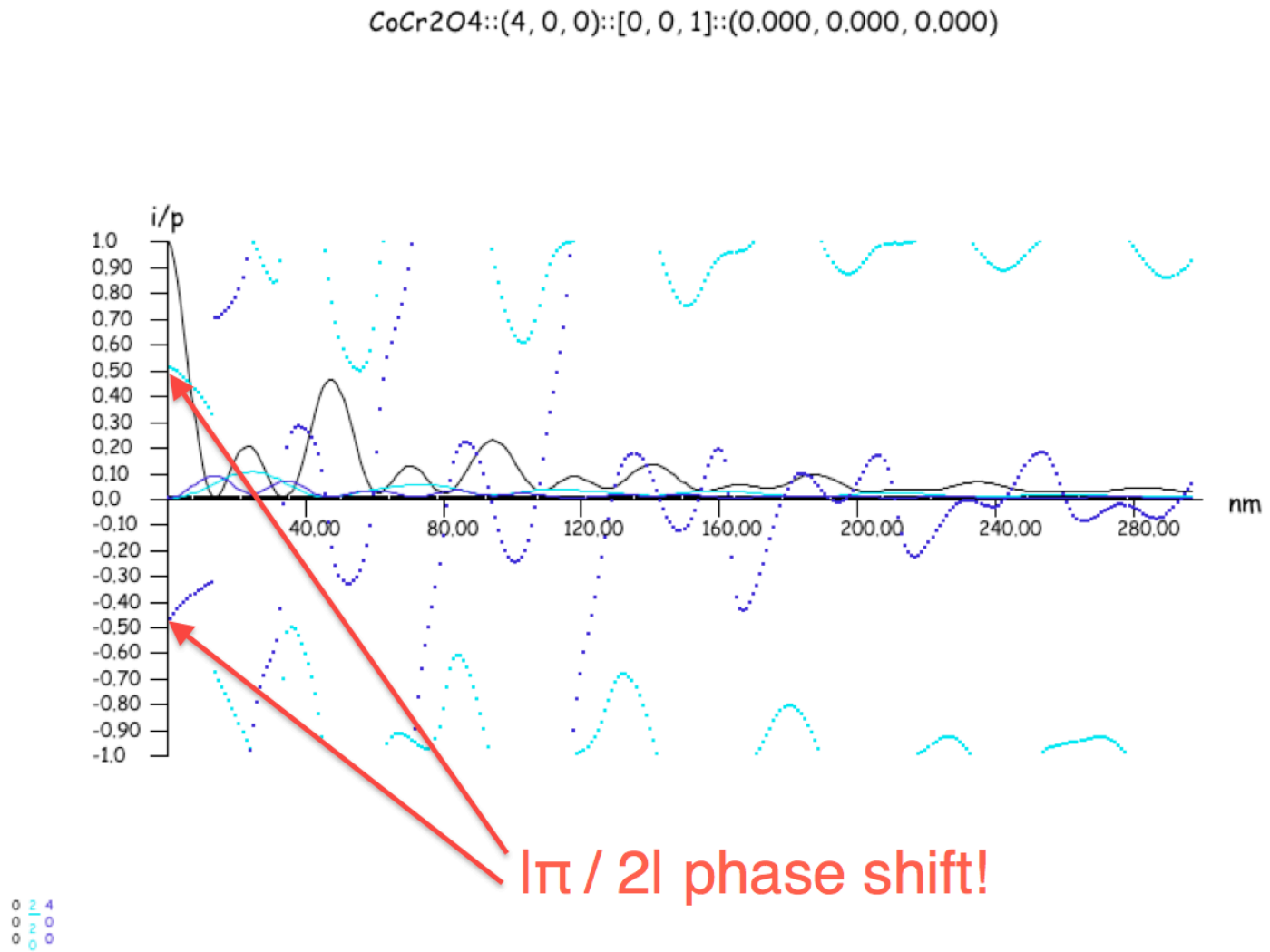

Dynamical scattering makes the amplitude & phase of transmitted (un-scattered) and reflections (scattered) beams vary widely as a function of specimen thickness (→ extinction distance).

Bloch wave method: applications

Simulation of:

- SAED (kinematical and dynamical).
- CBED (polarity).
- Channeling.
- LACBED (specimen thickness, symmetry).
- PED (Precession Electron Diffraction).
- HRTEM.

Works best for small lattice parameters crystals[4].

[4] Some more details during the labs.

CBED: ZnTe [110]

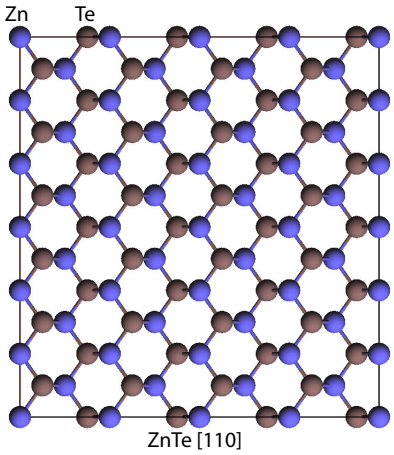

Figure: ZnTe [110].

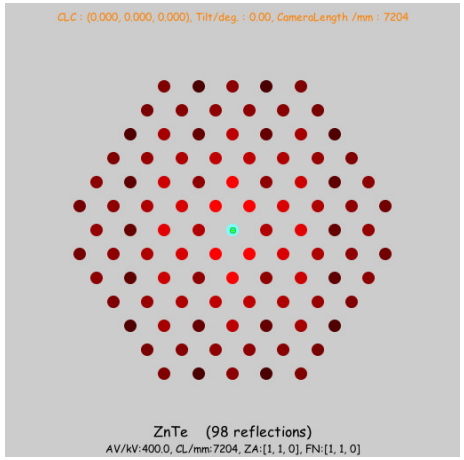

Figure: Reflections ($1 + 49$), $|\chi >= 0$.

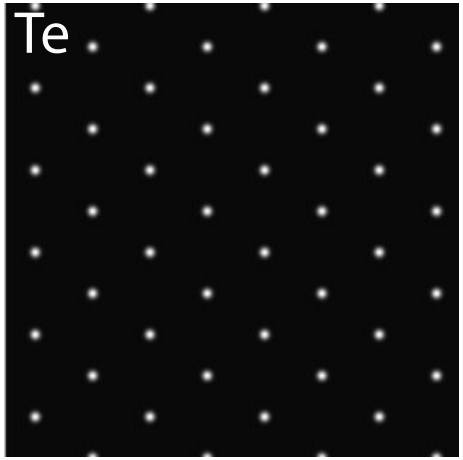

Figure: Bloch-wave 1 (Te 1s).

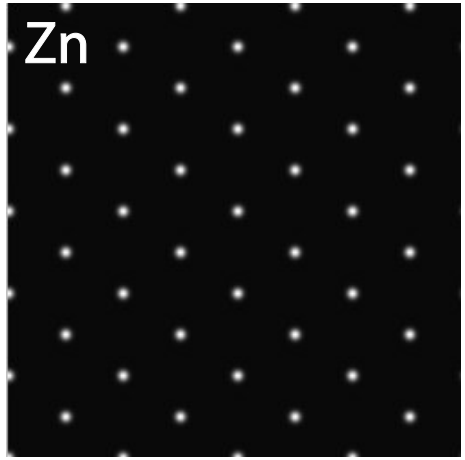

Figure: Bloch-wave 2 (Zn 1s).

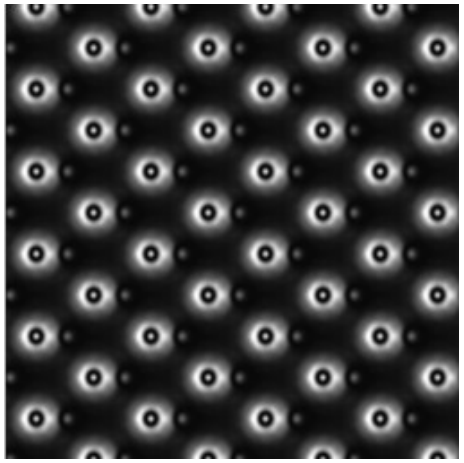

Figure: Bloch-wave 5 (Te-Zn).

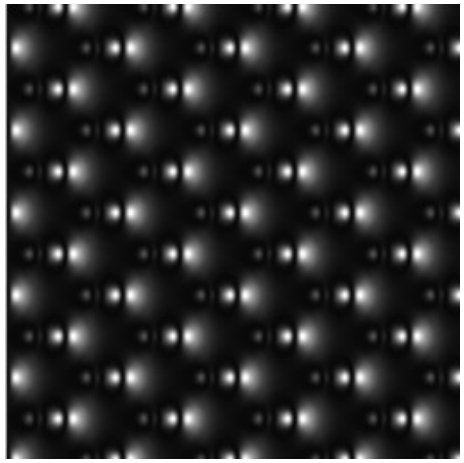

Figure: Bloch-wave 7 (Te-Zn).

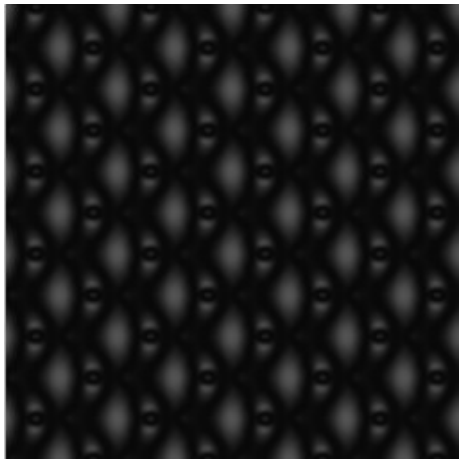

Figure: Bloch-wave 8 (Te-Zn).

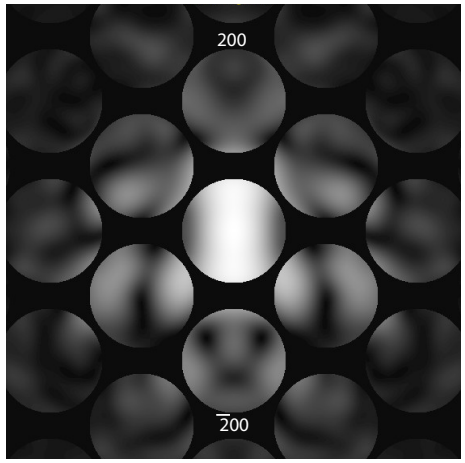

Figure: CBED (ZnTe polarity).

Electron channeling (ZnTe [110])

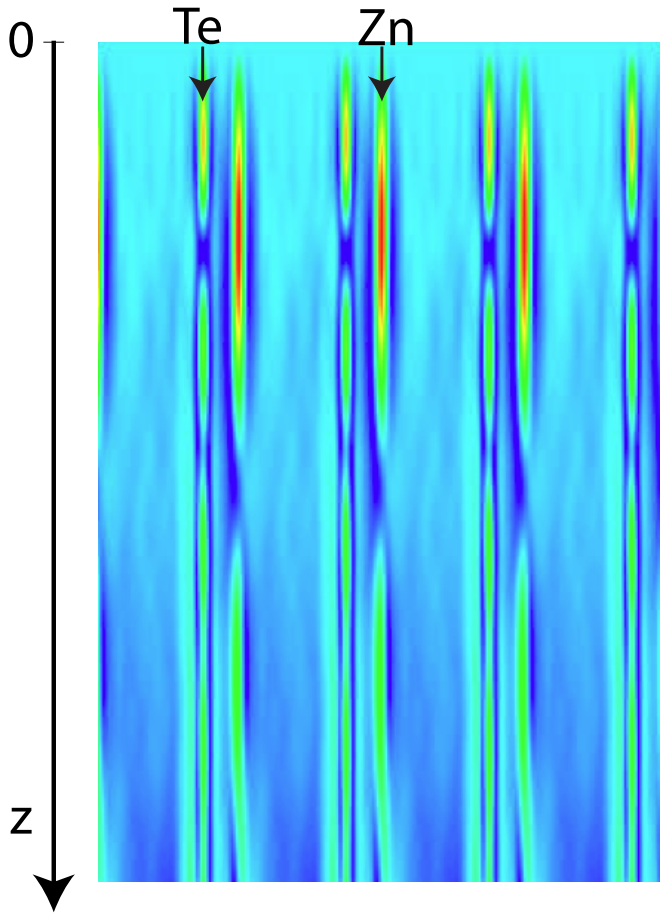

Figure: ZnTe [110] wave function intensity.

Channeling explains several features of HRTEM and STEM images:

- appearance / disappearance of contrast of impurities).
- dark (white) ring around atomic column in HRTEM images.

LACBED: Si [001]

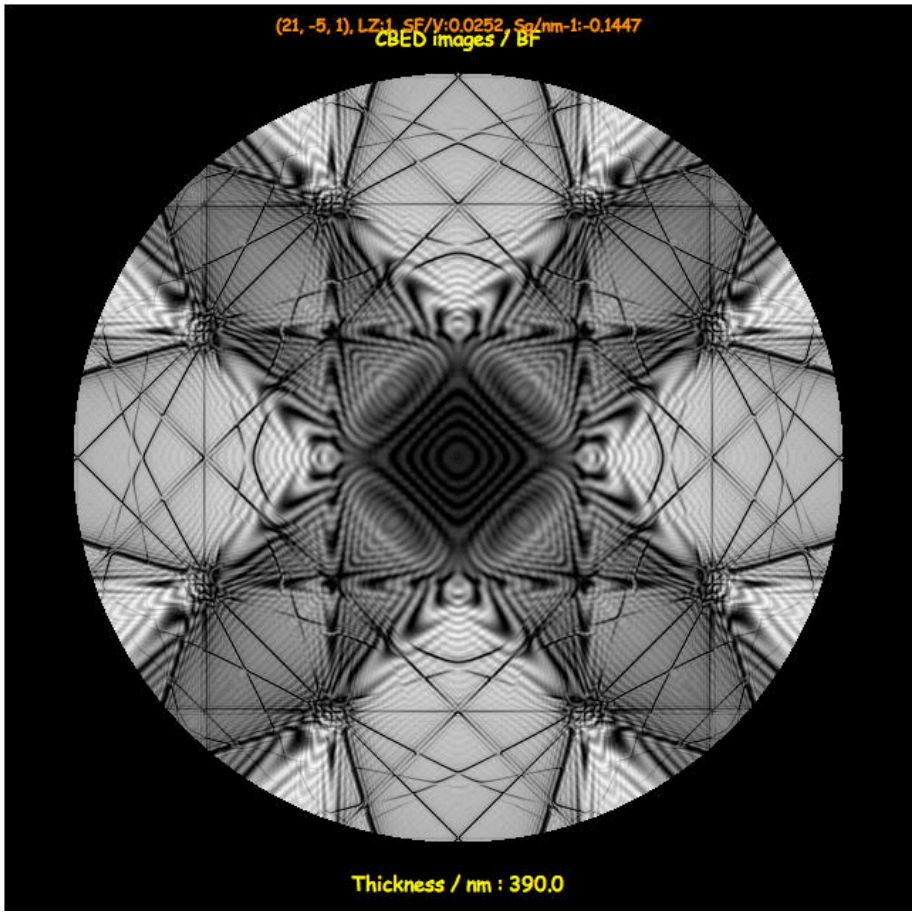

Figure: LACBED Si [001]: simulation.

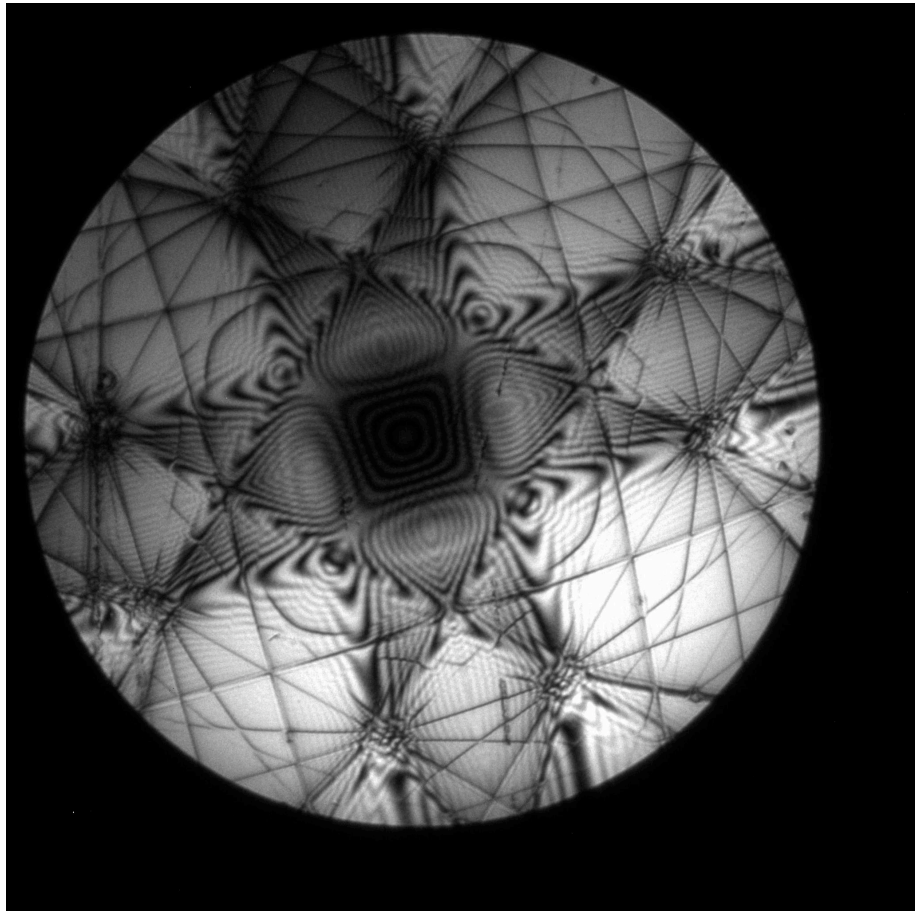

Figure: LACBED Si [001]: experimental (Web site EM centre - Monash university, J. Etheridge).

Note that the experimental LACBED pattern is blurred (inelastic scattering and/or MTF of CCD camera?).

Dynamical scattering calculations: multislice method

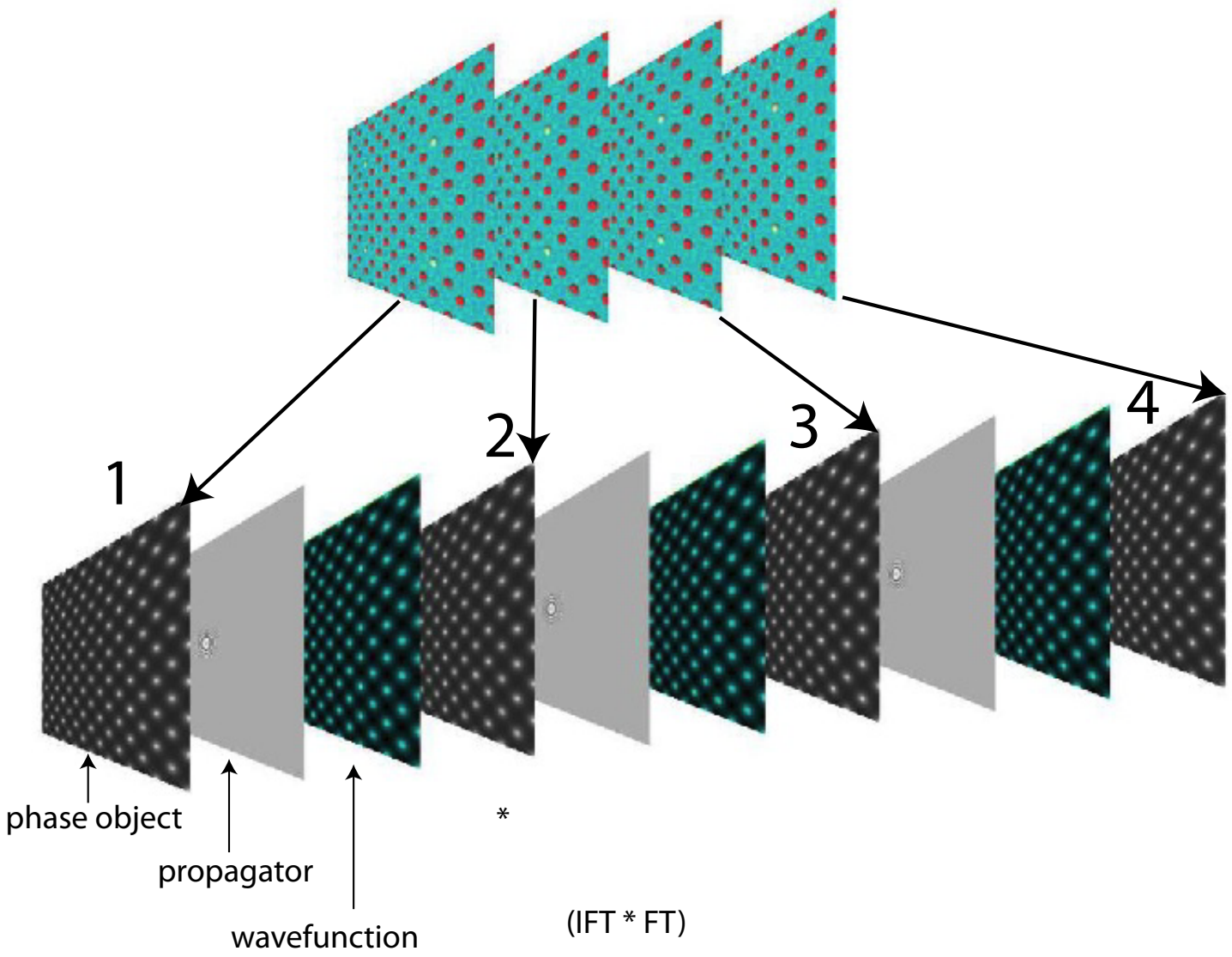

A very popular (and powerful) method for performing dynamical calculation has been proposed by J. M. Cowley and A.F. Moodie. It makes use of several principles of Optical Physics.

Multislice: slicing the crystal

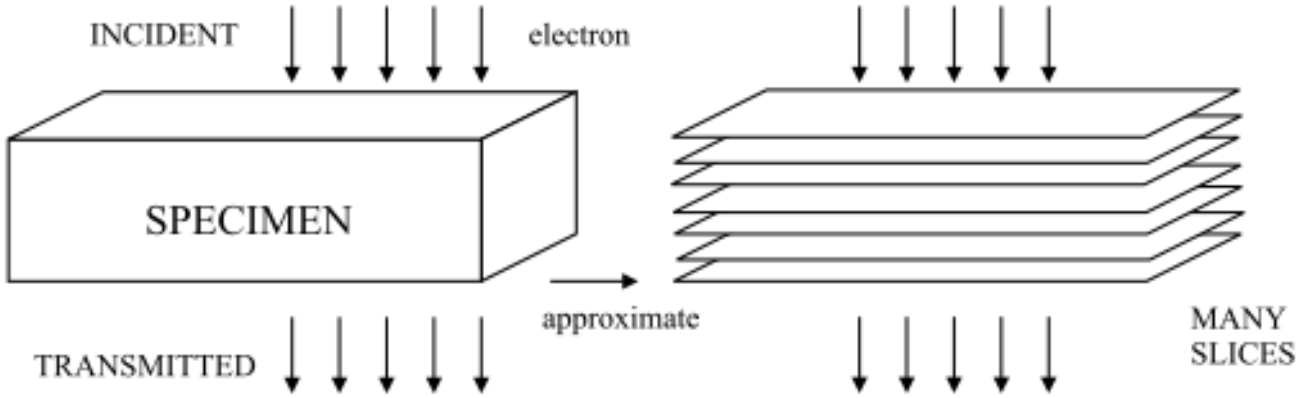

Figure: Crystal is sliced and the potential of the slices is projected on a plane.

Multislice: propagating the wave function

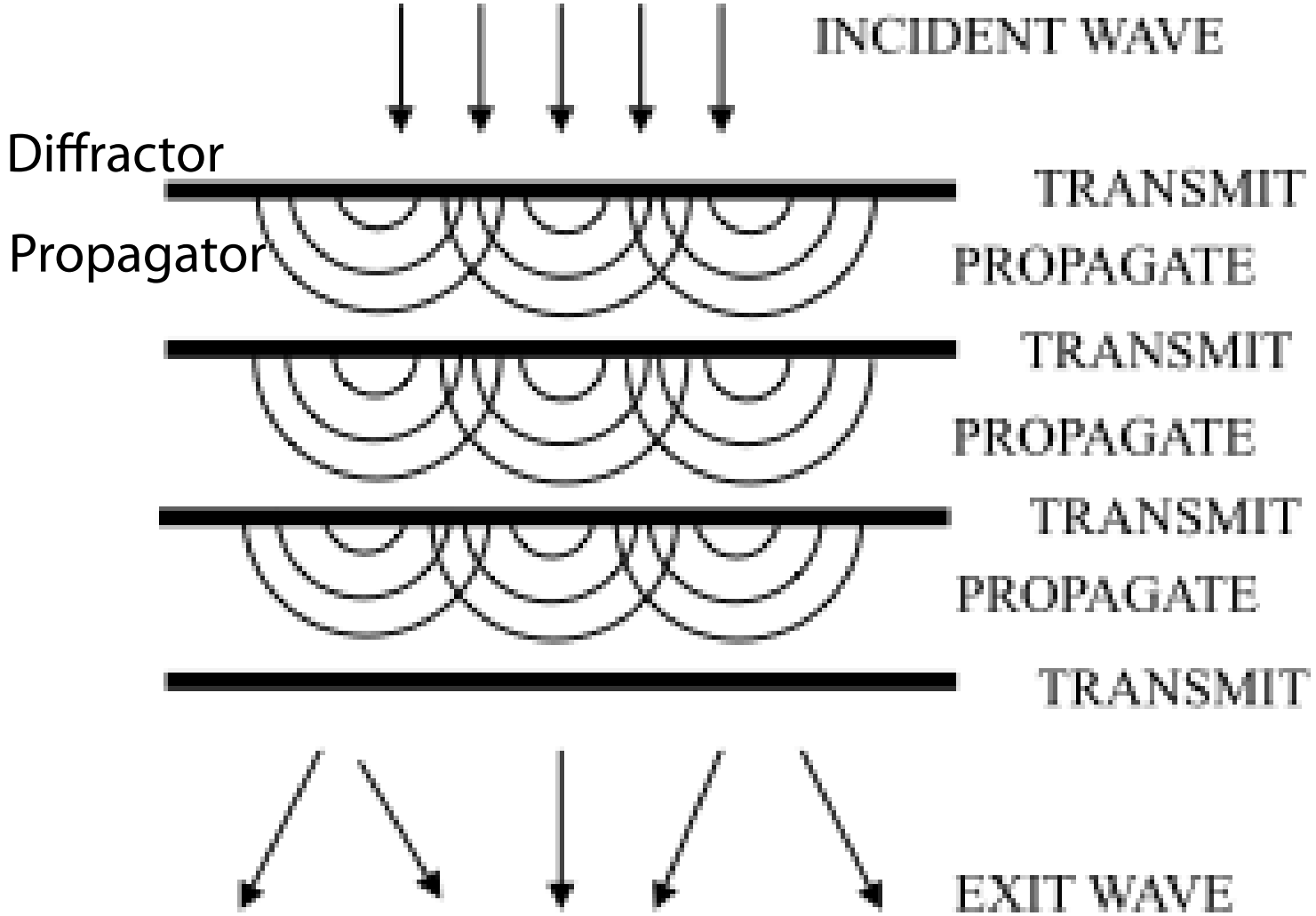

Figure: Wave function propagates through the stack of slices.

Multislice method: step 1 (AIN [1,1,1])

In order to define the slices (perpendicular to the optical axis), it is usually necessary to transform the crystal unit into an orthogonal cell (that can be pretty large).

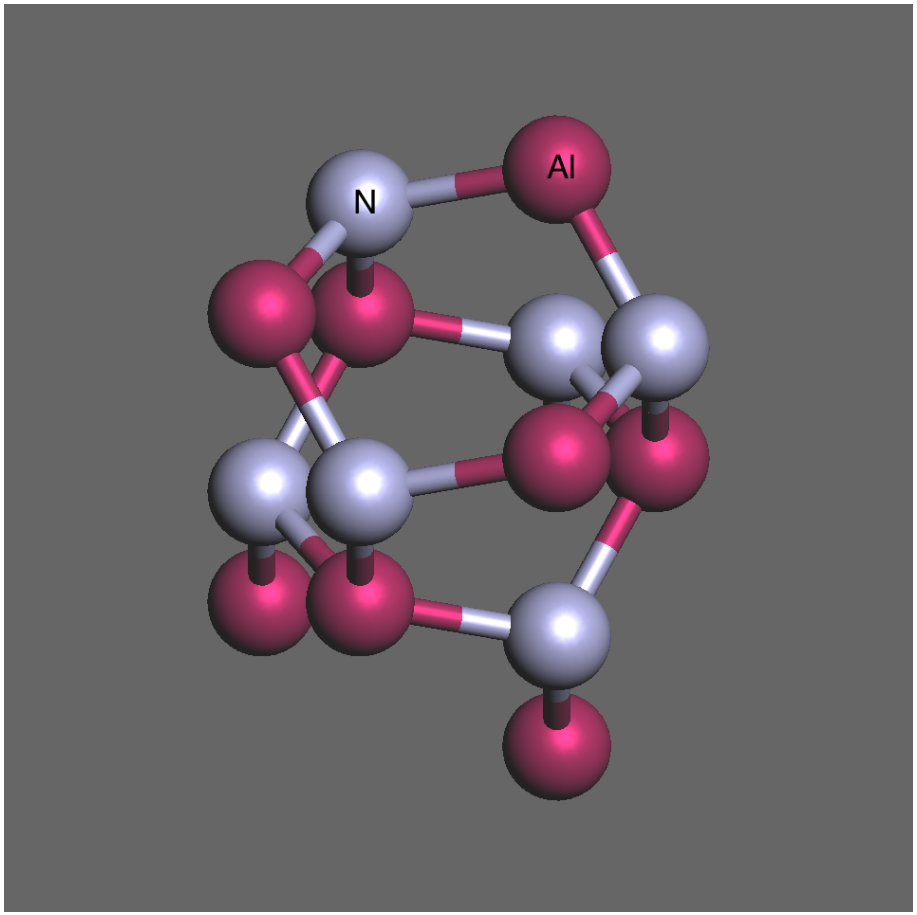

Model: AlN [1,1,1] projection (note the "*square*" groups of atoms).

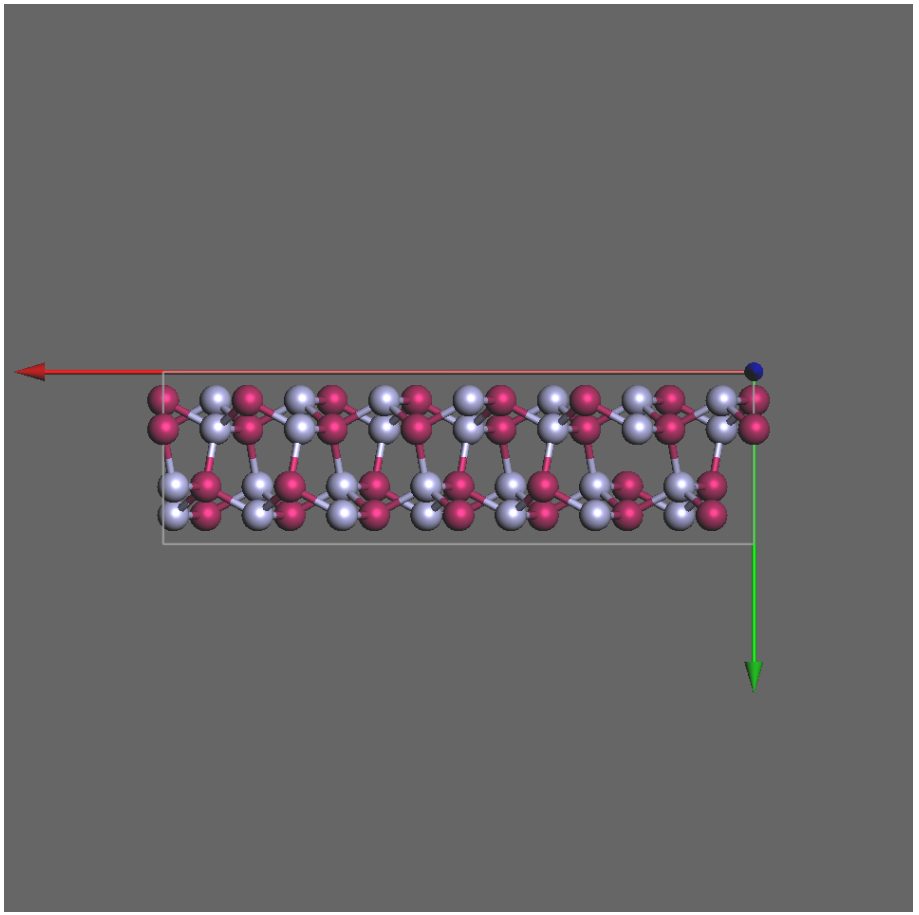

Transformed orthogonal AlN cell.

Step2: AlN [1,1,1] tetragonal slices

In order to define "*tetragonal*" slices (perpendicular to the optical axis), it is usually necessary to transform the crystal unit into an orthogonal cell (that can be pretty large).

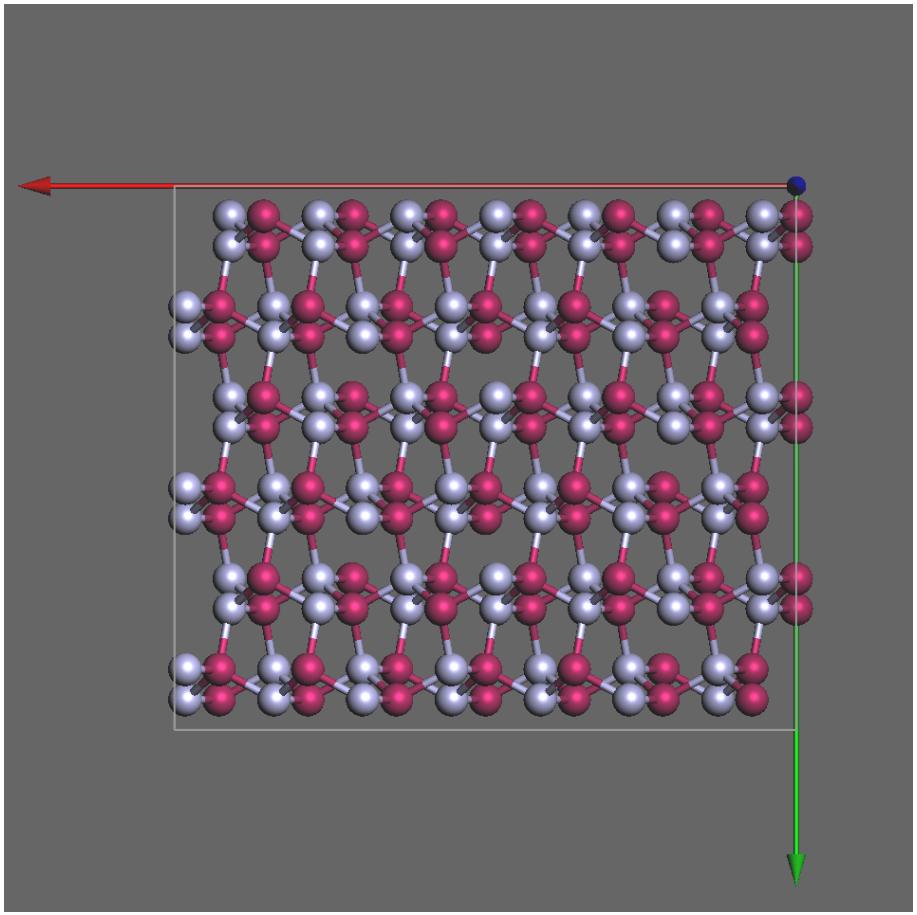

AlN [1,1,1] orthogonal unit cell duplicated to (almost) tetragonal unit cell.

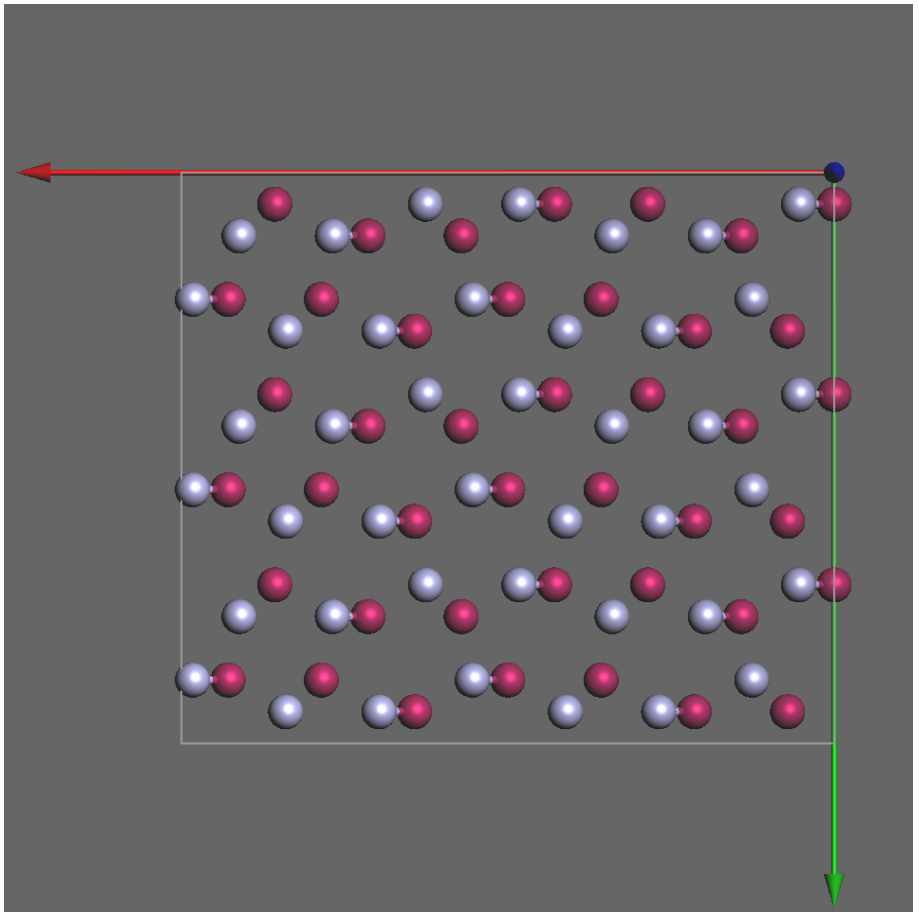

AlN [1,1,1] this slice ready for multislice calculation.

Step 3: projected potential & TDS potential

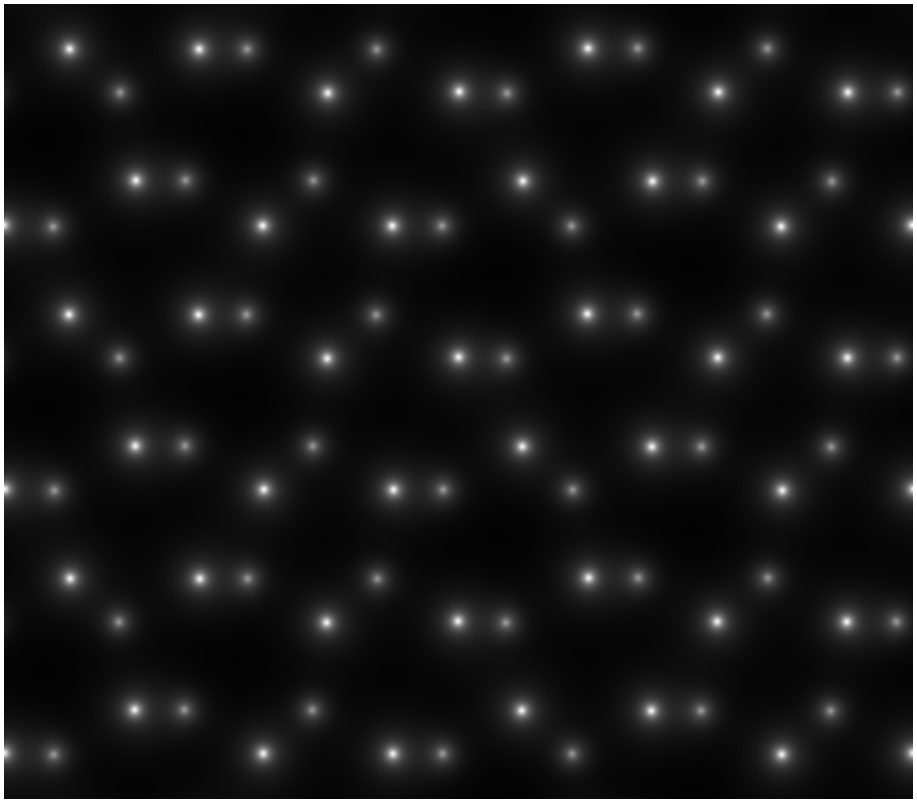

Projected potential slice 1.

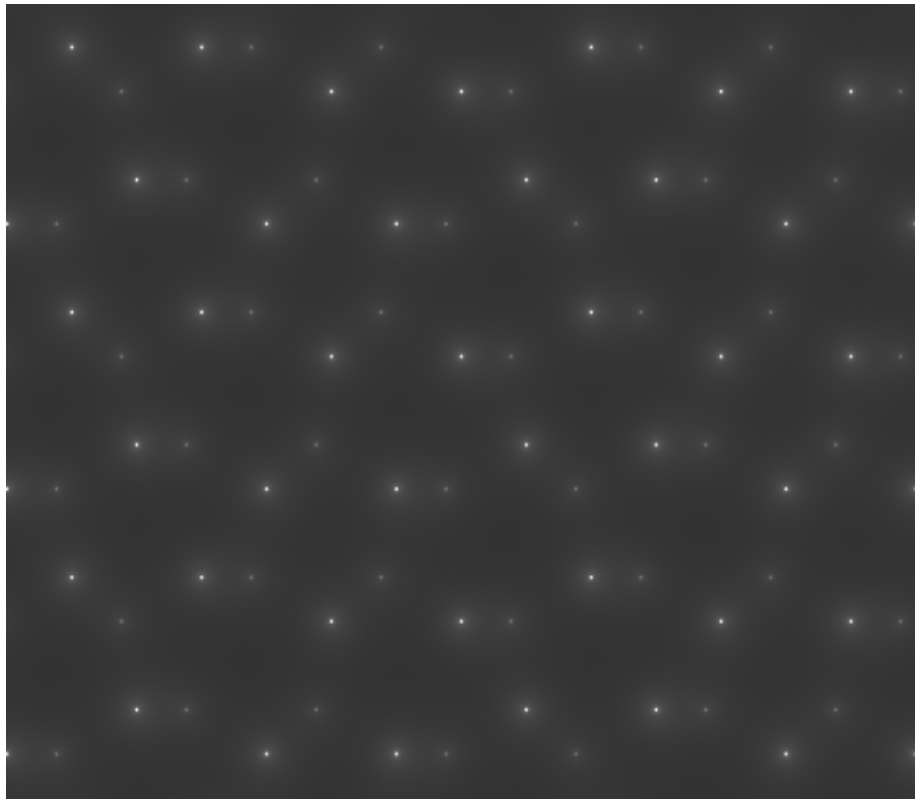

TDS potential slice 1.

Step 4: Phase object function: POF (x,y)

Phase object function slice 1 (real part).

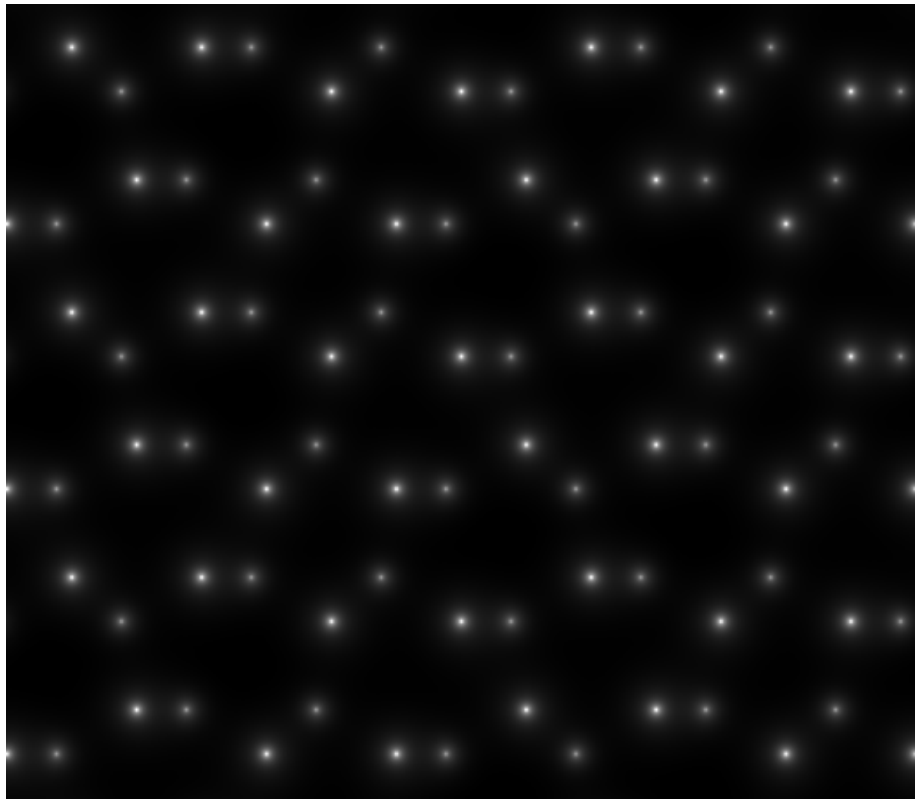

Phase object function slice 1 (imaginary part).

Step 5: Fresnel propagator: FP (x,y)

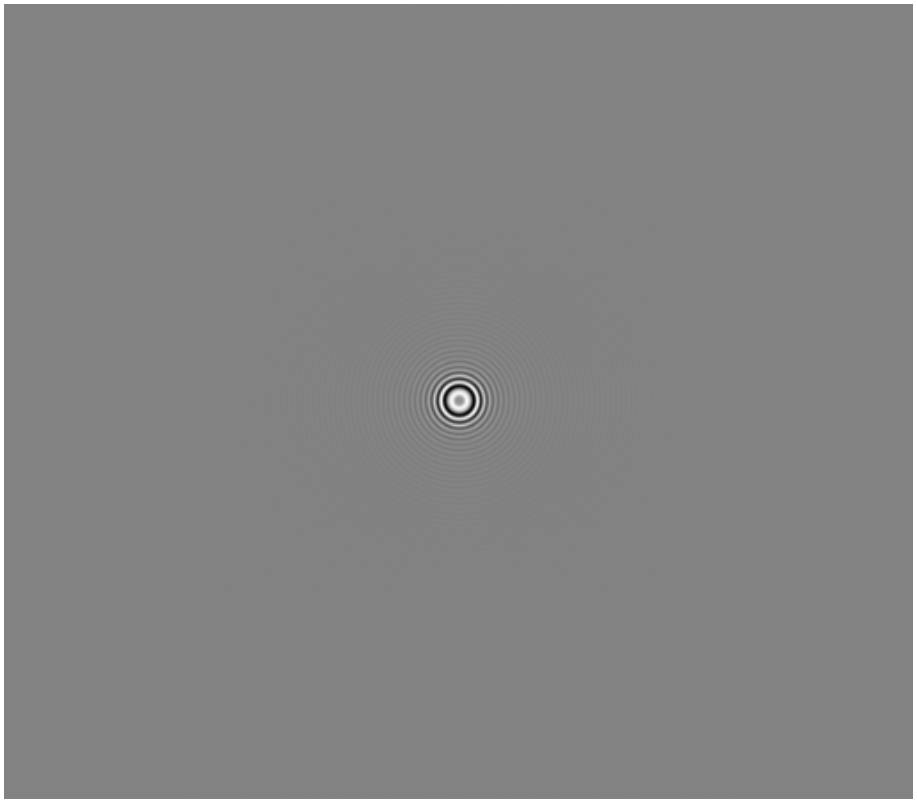

Fresnel propagator slice 1 (real part).

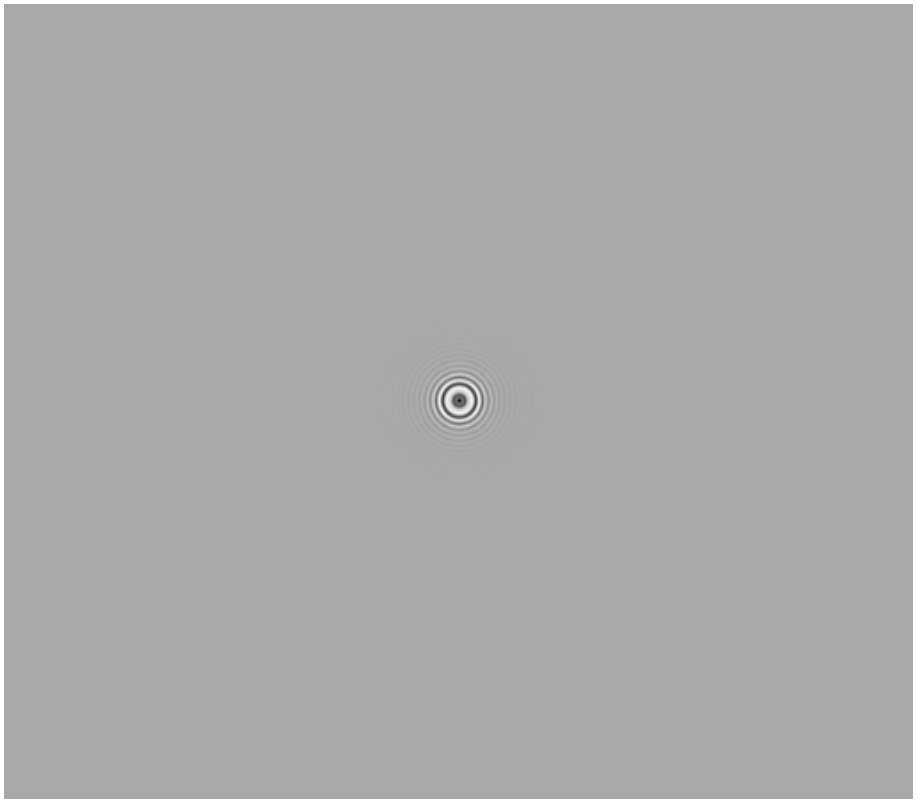

Fresnel propagator slice 1 (imaginary part).

Step 5: Fresnel propagator: $\widetilde{FP}(u, v)$

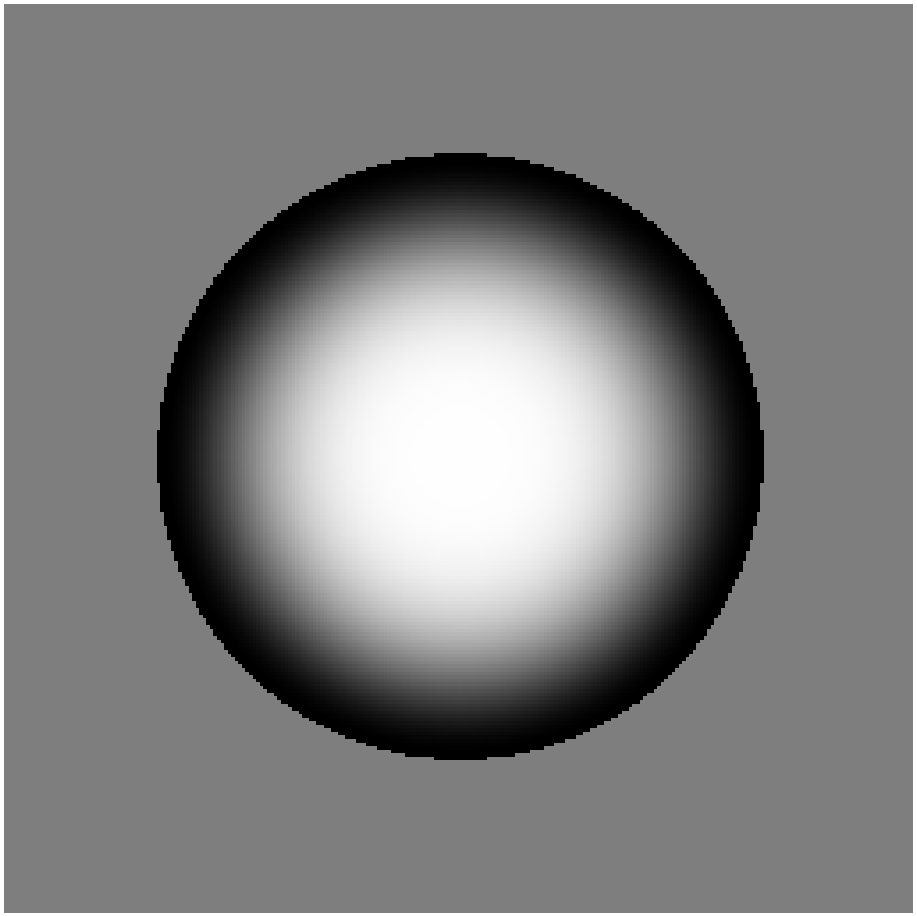

$FT\{Fresnel\ propagator\ slice1\}$ (real part).

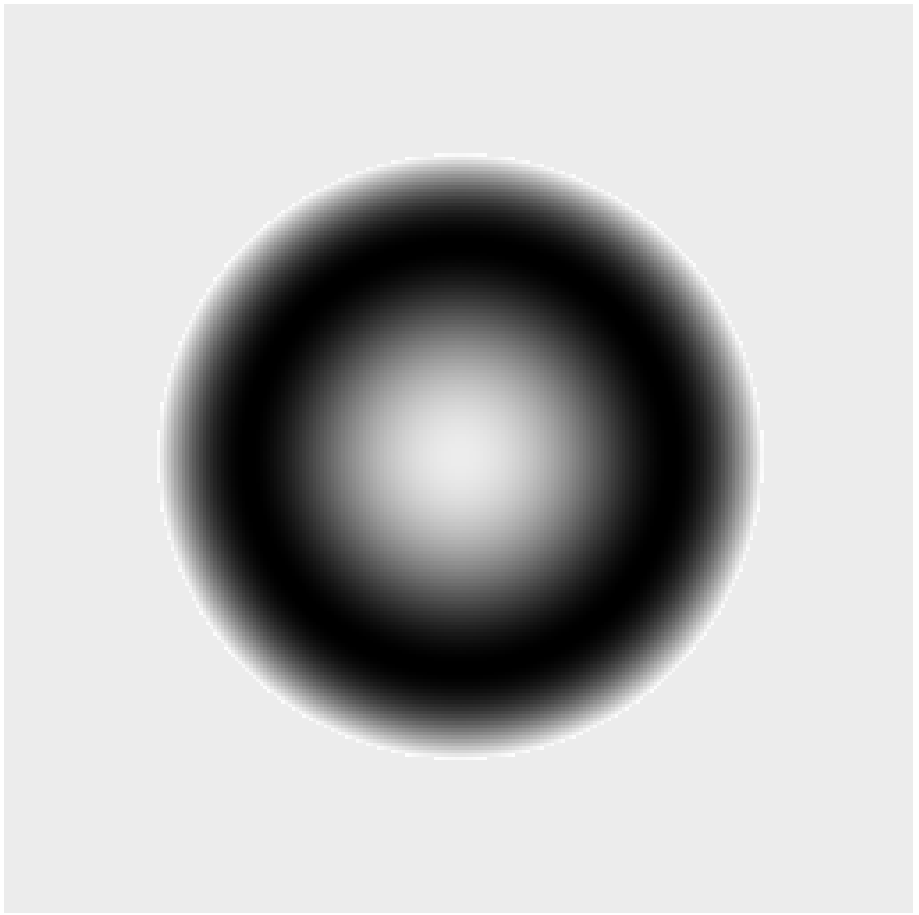

$FT\{Fresnel\ propagator\ slice1\}$ (imaginary part).

$$g(x) \otimes h(x) = FT^{-1}\left\{FT\{g(x)\} \times FT\{h(x)\}\right\} = FT^{-1}\left\{\widetilde{g}(u) \times \widetilde{h}(u)\right\}$$

Step 6: prepare the stack of AIN [1,1,1] slices

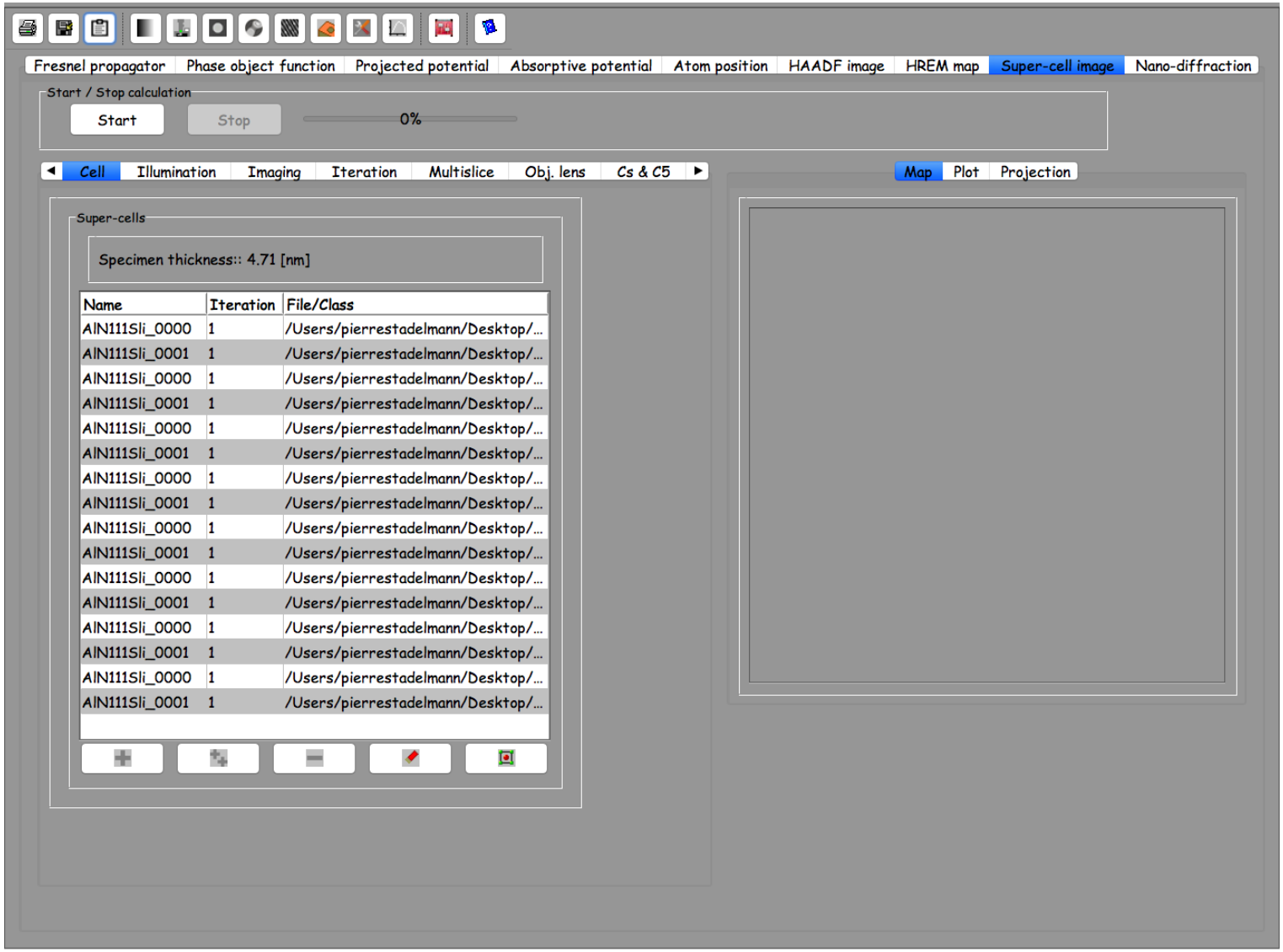

Stack of AIN [1,1,1] slices

Note that slices do not have to repeat. They can all be different.

Step 7: do the multislice iterations

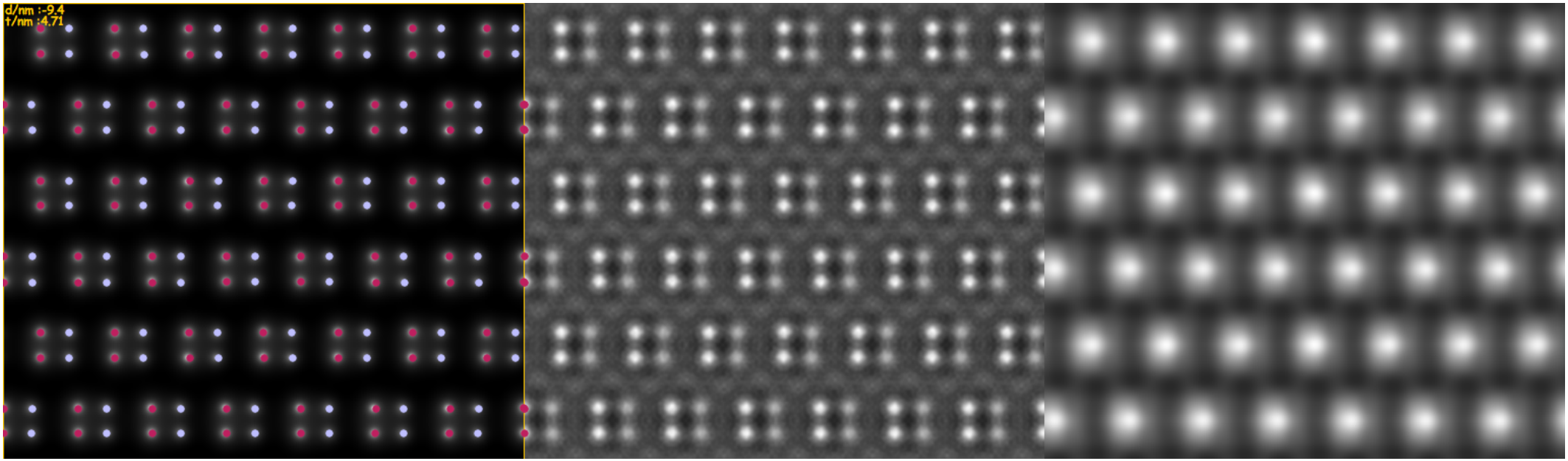

HRTEM AlN [1,1,1] (4.71 nm thick) (projected potential + atoms position, wave-function, image)

$$\Psi_{n+1}(x,y) = [\Psi_n(x,y) \otimes FP(x,y)]\, POF_{n+1}(x,y)$$

Dynamical scattering: bad and good

1. **Bad**
   - Phase relationship between transmitted and diffracted beams depends on thickness → HRTEM lattice fringes or contraste not always on atomic column position.
   - Amplitude of transmitted and diffracted beams depends on thickness → Some HRTEM lattice fringes may be missing or supplementary ones present.
2. **Good**
   - Specimen thickness can be determined precisely (~1 nm or better).
   - Specimen polarity can be determined.
   - Specimen deformation can be determined precisely.

Imaging

$$|\Psi_i> = \underbrace{\sum^{q'} <\rho|q'>}_{\text{Fourier synthesis}} \underbrace{\sum^{q} <q'|T(q',q)|q>}_{\text{Objective lens transfer}} \underbrace{<q|\widehat{U}(z,0)|\chi>}_{\text{Fourier transform}}$$

TEM and STEM image formation

1. Ray optics (remainder).
2. Perfect optical system.
3. Aberrations (spherical).
4. Properties of optical systems:
   - Linearity.
   - Space invariance.
5. Transfer function (coherent or partially coherent illumination - HRTEM).
6. Optical transfer function (incoherent illumination).

Optical system

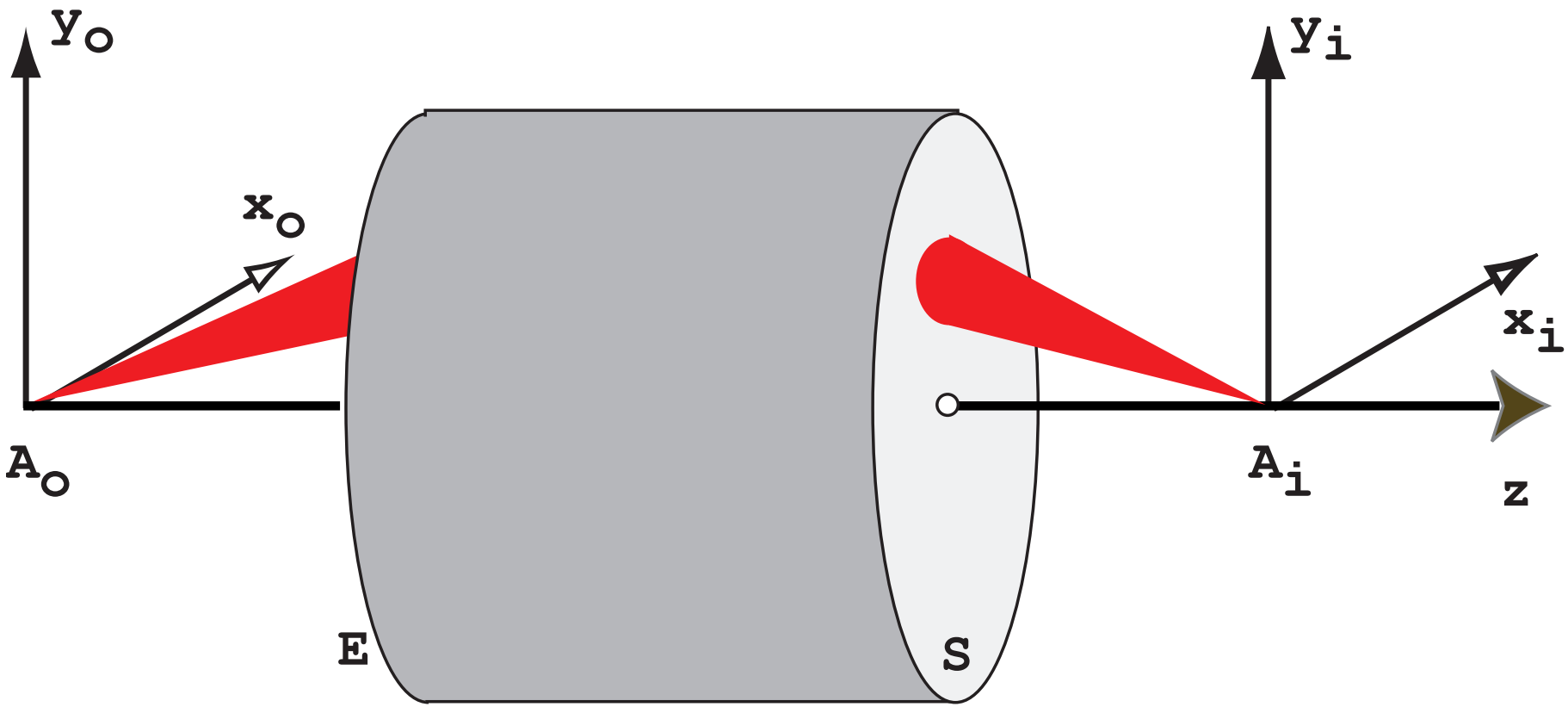

An optical system produces the image A_i of a point source object A_o. A_o and A_i are said to be conjugate. A_i is not a point since any optical system is diffraction limited. This limitation is introduced by the entrance and exit pupils of the optical system.

Important properties of optical system S

When the optical system has these **two** important properties:

1. Linearity.
2. Space invariance.

it can be globally characterized by a point spread function $t(\vec{x}-\vec{u})$.

$$\Psi_i(\vec{x}) = \int_{-\infty}^{\infty} \Psi_o(\vec{u}) t(\vec{x}-\vec{u}) \mathrm{d}\vec{u} = \Psi_o(\vec{x}) \otimes t(\vec{x})$$

Transfer function: property 1

Linearity

$$\begin{aligned} S\{a_1\Psi_o^1(\vec{x}) + a_2\Psi_o^2(\vec{x})\} &= a_1 S\{\Psi_o^1(\vec{x})\} + a_2 S\{\Psi_o^2(\vec{x})\} \\ S\{a_1\Psi_o^1(\vec{x}) + a_2\Psi_o^2(\vec{x})\} &= a_1\Psi_i^1(\vec{x}) + a_2\Psi_i^2(\vec{x}) \end{aligned}$$

Linearity allows to decompose the object wave-function in ∞ sum of point sources:

$$\Psi_o(\vec{x}) = \int_{-\infty}^{\infty} \Psi_o(\vec{\zeta})\delta(\vec{x}-\vec{\zeta})\mathrm{d}\vec{\zeta}$$

Image wave-function $\Psi_i(\vec{x})$:

$$\Psi_i(\vec{x}) = S\left\{\int_{-\infty}^{\infty} \Psi_o(\vec{\zeta})\delta(\vec{x}-\vec{\zeta})\mathrm{d}\vec{\zeta}\right\} = \int_{-\infty}^{\infty} \Psi_o(\vec{\zeta}) S\{\delta(\vec{x}-\vec{\zeta})\}\mathrm{d}\vec{\zeta}$$

$$\Psi_i(\vec{x}) = \int_{-\infty}^{\infty} \Psi_o(\vec{\zeta})\, T(\vec{x};\vec{\zeta})\mathrm{d}\vec{\zeta}$$

where $T(\vec{x};\vec{\zeta}) = S\{\delta(\vec{x}-\vec{\zeta})\}$: **Impulse Response** of optical system S.

Transfer function: property 2

Space invariance

Space invariance is realised when the image of a point source is independent of its position in the object plane, i.e. when the point source moves in the object plane its image moves similarly in the image plane without changing form and intensity.

$$T(\vec{x};\vec{\zeta}) = T(\vec{x}-\vec{\zeta})$$

$$\Psi_i(\vec{x}) = \int_{-\infty}^{\infty} \Psi_o(\vec{\zeta})\, T(\vec{x}-\vec{\zeta})\mathrm{d}\vec{\zeta} = \Psi_o(\vec{x}) \otimes T(\vec{x})$$

Convolution integral spreads object information, degrades performance of optical system.

In Fourier space:

$$\widetilde{\Psi}_i(\vec{q}) = \widetilde{\Psi}_o(\vec{q})\, \widetilde{T}(\vec{q})$$

$\widetilde{T}(\vec{q})$: transfer function of optical system.

Summary: point spread function $t(\vec{x})$ and transfer function $\widetilde{T}(\vec{k})$

Transfer is a convolution integral of $\Psi_o(\vec{u})$ and the point spread function $t(\vec{u})$:

$$\Psi_i(\vec{x}) = \int_{-\infty}^{\infty} \Psi_o(\vec{u}) t(\vec{x} - \vec{u}) \mathrm{d}\vec{u} = \Psi_o(\vec{x}) \otimes t(\vec{x})$$

In Fourier space (or reciprocal space):

$$\widetilde{\Psi}_i(\vec{k}) = \widetilde{\Psi}_o(\vec{k}) \widetilde{T}(\vec{k})$$

Where $\widetilde{T}(\vec{k})$ is the transfer function of the microscope.

Pupils

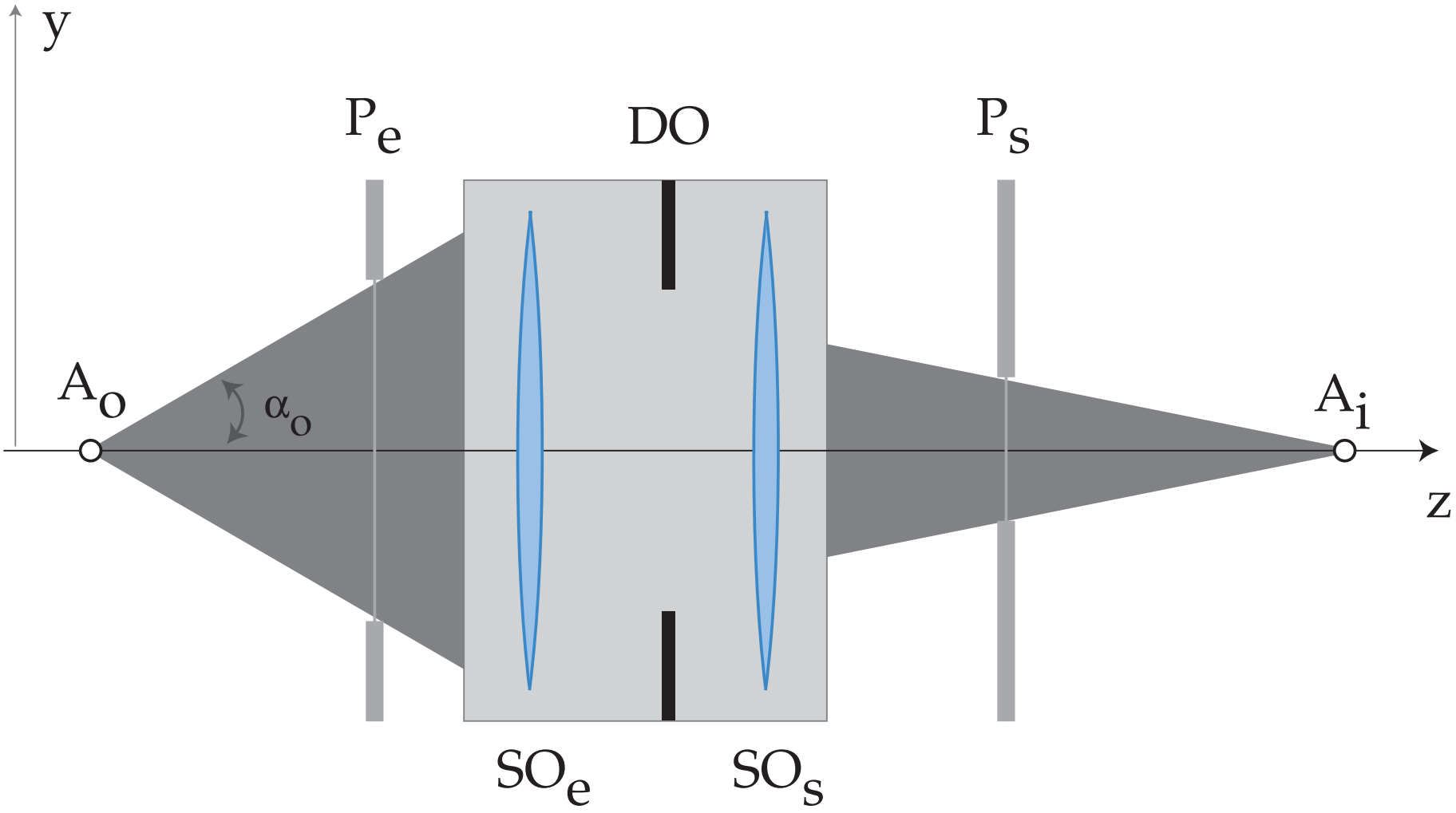

Any optical system can be characterised by an entrance pupil P_e and an exit pupil P_s. The pupils are the image of the opening aperture DO by the entrance and exit optical subsystems SO_e and SO_s. A perfect optical system the spherical wave emitted in A_o into a portion of a perfect spherical wave due to the limited size of the pupils.

Aberrations of optical systems: how to define them

Position of $A_i \longrightarrow$ intersection of the reference light ray (non deviated) and the image plane.

Diffraction limited: some light rays emitted by object point A_o do not reach the image at point A_i. The image of a point source is a **spot** whose shape and intensity depend on the quality of the optical system.

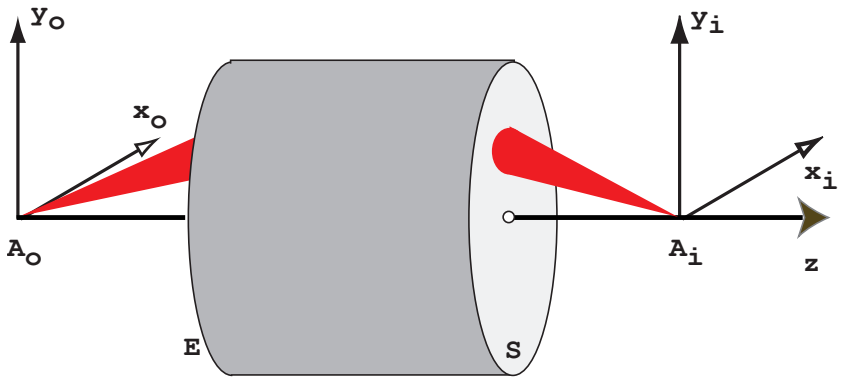

Two types of aberrations:

1. Monochromatic.
2. Chromatic (λ dependent).

Optical Path Length: OPL

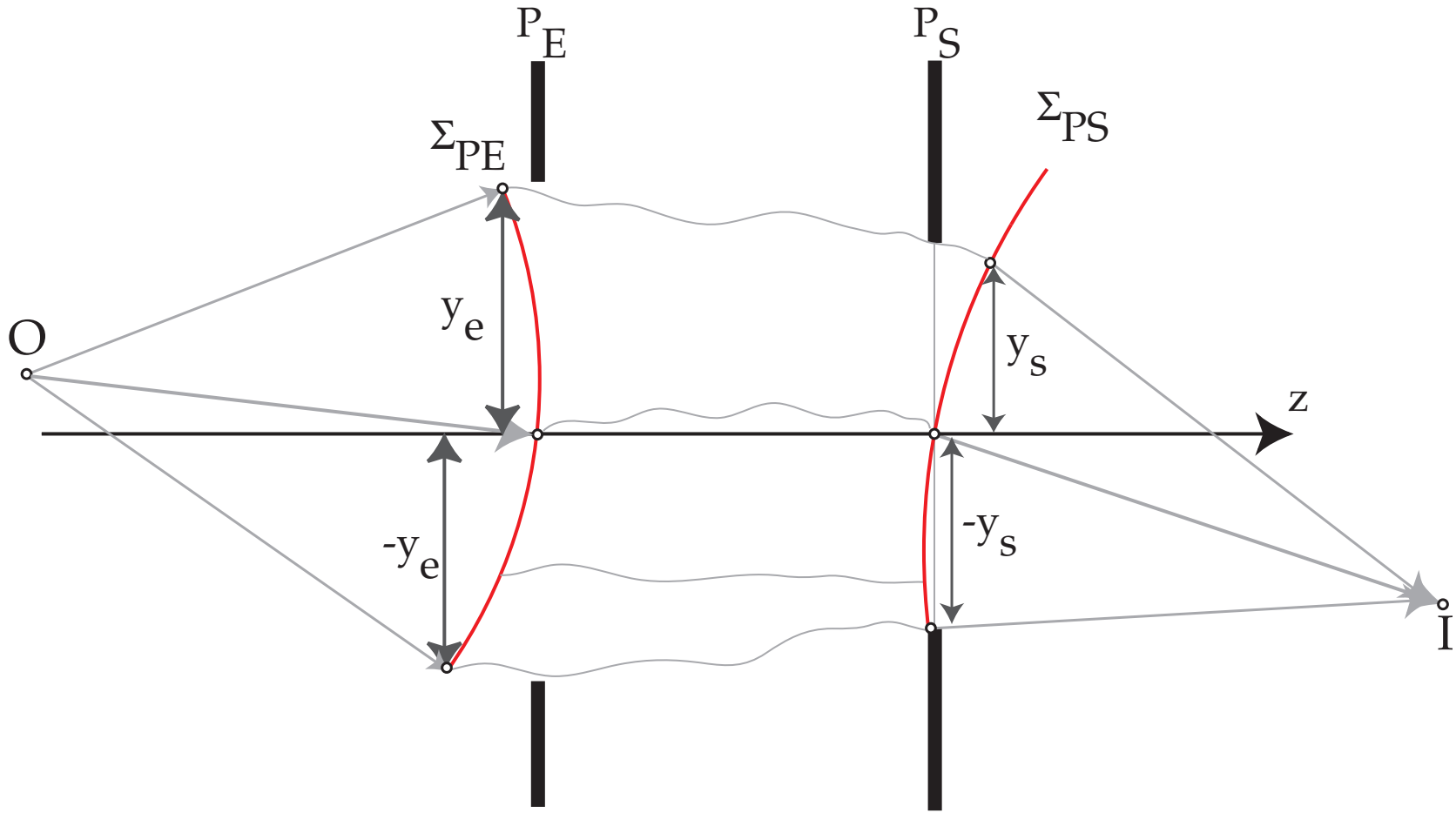

- Before P_E the reference wavefront Σ_{PE} is spherical (point source at O).
- After P_S the reference wavefront Σ_{PS} is spherical (converges towards I).

For a perfect optical system, both the entrance Σ_{PE} and exit Σ_{PS} wavefronts are spherical. The Optical Path Length form O to I is independent of the path.

Optical Path Difference (OPD): aberrations

In the presence of aberrations the wavefront $\Sigma_S^{'}$ is no more spherical.

The Optical Path Difference (distance between the deformed $\Sigma_S^{'}$ and spherical wavefront Σ_S) introduces a phase shift $\delta\phi$.

With P' close to $P = (x_s, y_s)$ on reference sphere Σ_s, the OPD at P' = (i.e. OPL from P' to P) is given by (Fermat principle):

$$W(x_s, y_s) = n_i \overline{P'P}$$

n_i refractive index of the medium $\longrightarrow$ **phase shift**:

$$\delta\phi = e^{2\pi\imath \frac{W(x_s, y_s)}{\lambda}}$$

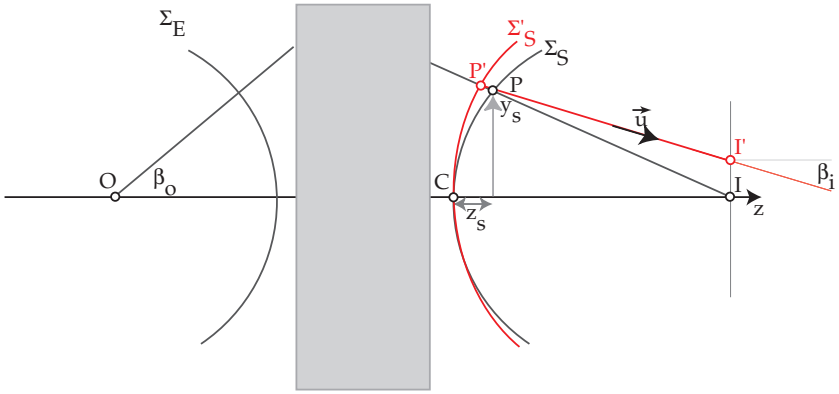

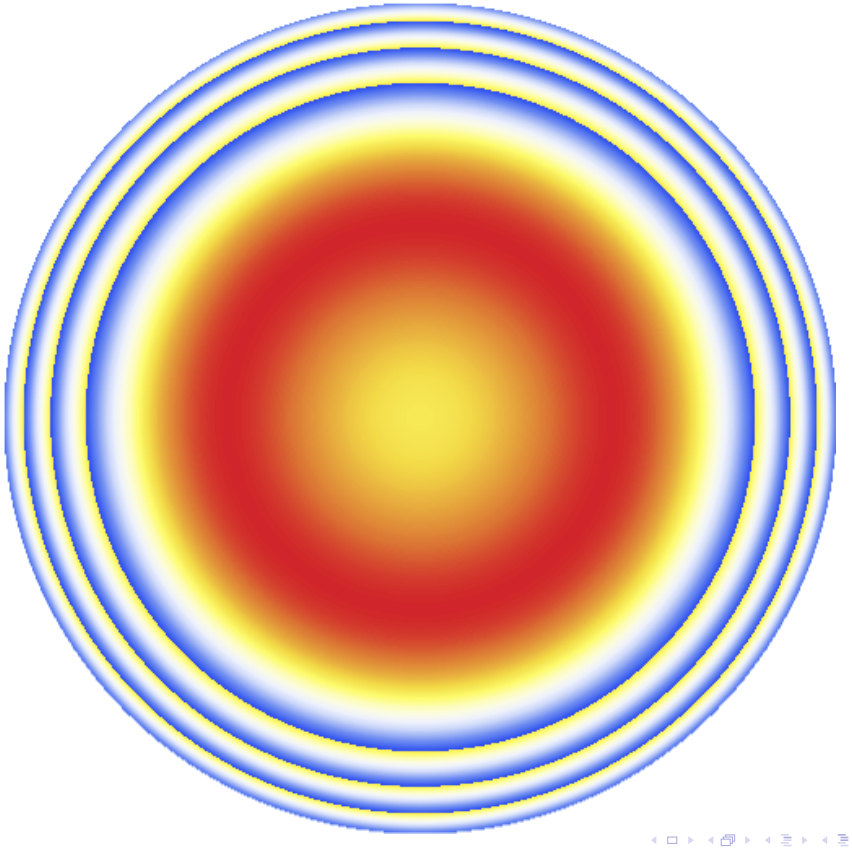

Transverse geometric aberrations: $\vec{\epsilon}$

The transverse geometric aberrations are proportional to $\frac{d}{d\theta}$ wavefront aberrations[5]:

$$\epsilon_x = -\frac{f}{n_i}\frac{\partial W}{\partial x_s}$$
$$\epsilon_y = -\frac{f}{n_i}\frac{\partial W}{\partial y_s}$$

f focal length.

The OPD's introduced by all the aberrations of the imaging system are collected in a function $\chi(\vec{u})$ and the phase shift is[6]:

$$\widetilde{T}(\vec{u}) = e^{\imath\chi(\vec{u})}$$

$\widetilde{T}(\vec{u})$ has been first employed by Abbe in his description of image formation (1866).

[5] $P(x_s, y_s)$ on the spherical reference wavefront can be characterised by the radial angle θ.

[6] The angle θ corresponds (through Bragg law) to a spatial frequency $\vec{u}$, i.e. a distance in the back focal plane.

Wavefront aberrations (to 6^{th} order) in cartesian coordinates

$$\{W(1,1) \rightarrow 2\pi(u\cos(\phi(1,1)) + v\sin(\phi(1,1)))\}\ (\textit{image shift})$$
$$\{W(2,0) \rightarrow \pi\left(u^2+v^2\right)\lambda\}\ (\textit{defocus})$$
$$\{W(2,2) \rightarrow \pi\lambda((u-v)(u+v)\cos(2\phi(2,2)) + 2uv\sin(2\phi(2,2)))\}\ (\textit{two-fold astigmatism})$$
$$\{W(3,1) \rightarrow \tfrac{2}{3}\pi\left(u^2+v^2\right)\lambda^2(u\cos(\phi(3,1)) + v\sin(\phi(3,1)))\}\ (\textit{coma})$$
$$\{W(3,3) \rightarrow \tfrac{2}{3}\pi\lambda^2\left(u\left(u^2-3v^2\right)\cos(3\phi(3,3)) - v\left(v^2-3u^2\right)\sin(3\phi(3,3))\right)\}\ (\textit{three-fold astigmatism})$$
$$\left\{W(4,0) \rightarrow \tfrac{1}{2}\pi\left(u^2+v^2\right)^2\lambda^3\right\}(\textit{spherical aberration})$$
$$\{W(4,2) \rightarrow \tfrac{1}{2}\pi\left(u^2+v^2\right)\lambda^3((u-v)(u+v)\cos(2\phi(4,2)) + 2uv\sin(2\phi(4,2)))\}$$
$$\{W(4,4) \rightarrow \tfrac{1}{2}\pi\lambda^3\left(\left(u^4-6v^2u^2+v^4\right)\cos(4\phi(4,4)) + 4u(u-v)v(u+v)\sin(4\phi(4,4))\right)\}$$
$$\left\{W(5,1) \rightarrow \tfrac{2}{5}\pi\left(u^2+v^2\right)^2\lambda^4(u\cos(\phi(5,1)) + v\sin(\phi(5,1)))\right\}$$
$$\{W(5,3) \rightarrow \tfrac{2}{5}\pi\left(u^2+v^2\right)\lambda^4\left(u\left(u^2-3v^2\right)\cos(3\phi(5,3)) - v\left(v^2-3u^2\right)\sin(3\phi(5,3))\right)\}$$
$$\{W(5,5) \rightarrow \tfrac{2}{5}\pi\lambda^4\left(u\left(u^4-10v^2u^2+5v^4\right)\cos(5\phi(5,5)) + v\left(5u^4-10v^2u^2+v^4\right)\sin(5\phi(5,5))\right)\}$$
$$\left\{W(6,0) \rightarrow \tfrac{1}{3}\pi\left(u^2+v^2\right)^3\lambda^5\right\}$$
$$\left\{W(6,2) \rightarrow \tfrac{1}{3}\pi\left(u^2+v^2\right)^2\lambda^5((u-v)(u+v)\cos(2\phi(6,2)) + 2uv\sin(2\phi(6,2)))\right\}$$
$$\{W(6,4) \rightarrow \tfrac{1}{3}\pi\lambda^5\left(\left(u^6-5v^2u^4-5v^4u^2+v^6\right)\cos(4\phi(6,4)) + 4uv\left(u^4-v^4\right)\sin(4\phi(6,4))\right)\}$$
$$\{W(6,6) \rightarrow \tfrac{1}{3}\pi\lambda^5\left(\left(u^6-15v^2u^4+15v^4u^2-v^6\right)\cos(6\phi(6,6)) + 2uv\left(3u^4-10v^2u^2+3v^4\right)\sin(6\phi(6,6))\right)\}$$

Model: Abbe image formation

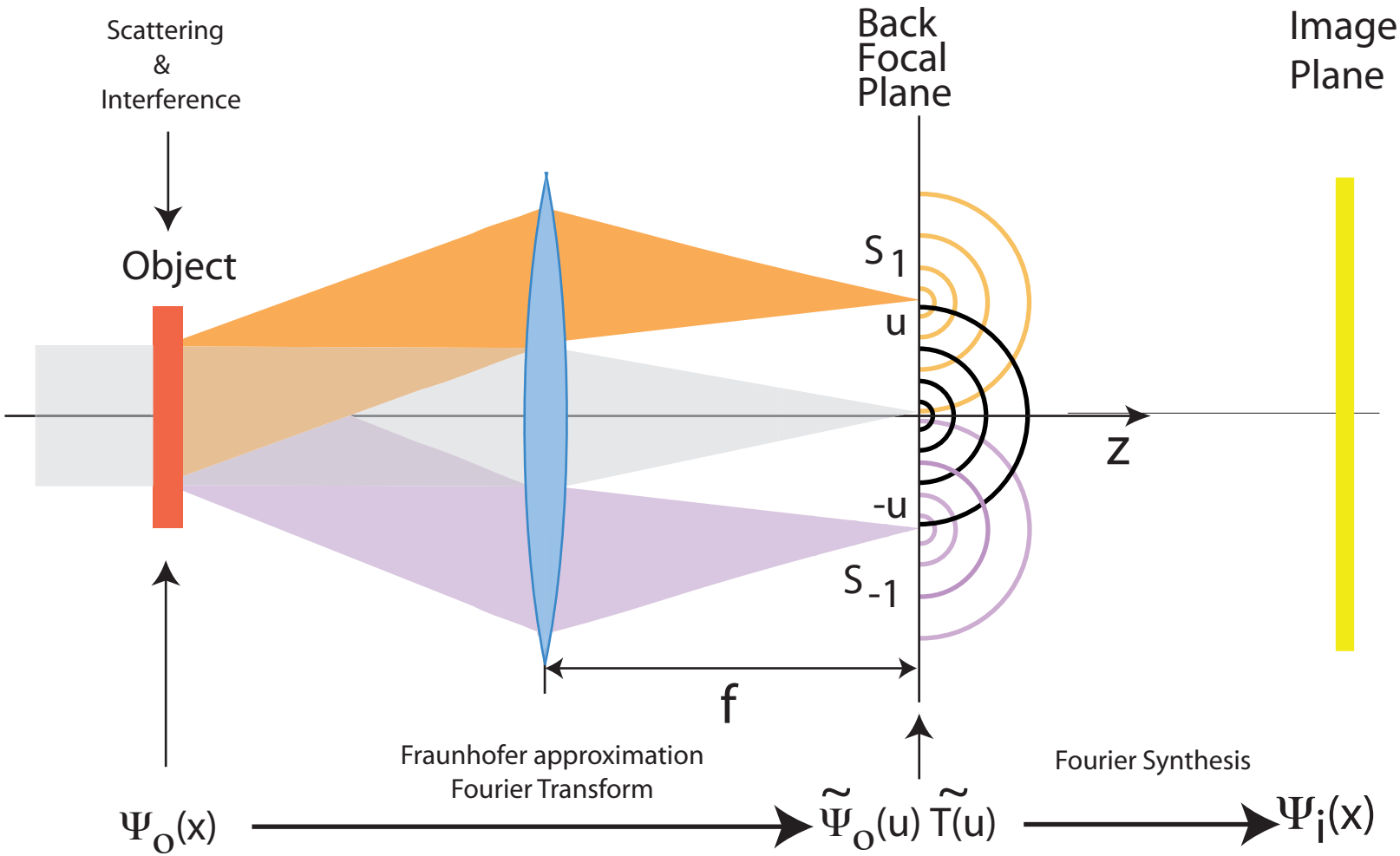

The objective lens changes the **phase relationship** between the transmitted and diffracted beams. Moreover not all diffracted beams are transmitted, due to its small acceptance angle. High spatial frequencies (i.e. beams diffracted at large angles are damped due to **partial spatial and temporal coherence**, electronic or thermal magnetic noise, mechanical vibrations, drift, ...).

$PSF(\vec{x}) = FT^{-1}\left[\widetilde{T}(\vec{h})\right]$ point spread function.

- Coherent illunination:

$$\Phi_i(\vec{x}) = \Phi_o(\vec{x}) \otimes PSF(\vec{x})$$

- Partially coherent illumination:

$$\widetilde{I}(\vec{h}; z) = \int \widetilde{T}_{cc}(\vec{h}' + \vec{h}; \vec{h}; z)\phi(\vec{h}' + \vec{h})\phi^*(\vec{h}')\mathrm{d}\vec{h}'$$

- Incoherent illumination:

$$I(\vec{x}) = |\Phi_o(\vec{x})|^2 \otimes [PSF(\vec{x})PSF^*(-\vec{x})]$$

HRTEM

coherent or partially coherent image formation process with coherent or partially coherent incident wave.

TEM ($\widetilde{T}(\vec{q})$: Transfer Function):

$$\widetilde{\Psi}_i(\vec{q}) = \widetilde{\Psi}_o(\vec{q})\widetilde{T}(\vec{q})$$
$$\Psi_i(\vec{x}) = \int \widetilde{\Psi}_o(\vec{q})\widetilde{T}(\vec{q})e^{2\pi\imath\vec{q}\cdot\vec{x}}\mathrm{d}\vec{q}$$

HRSTEM

Incoherent image formation process with coherent or partially coherent probe.

STEM ($\widetilde{OTF}(\vec{q}) = \widetilde{T}(\vec{q}) \otimes \widetilde{T}(-\vec{q})$: Optical Transfer Function):

$$
\begin{array}{lcll}
I(\vec{x}) & = & \langle \Psi_i(\vec{x};t)\Psi_i^*(\vec{x};t)\rangle & \text{(time average)} \\
\Psi_i(\vec{x};t) & = & \Psi_o(\vec{x};t) \otimes T(\vec{x}) & (T(\vec{x}) : \text{PSF independent of t}) \\
I(\vec{x}) & = & \langle [\Psi_o(\vec{x};t) \otimes T(\vec{x})][\Psi_o^*(\vec{x};t) \otimes T^*(\vec{x})]\rangle & (\otimes \text{ convolution.}) \\
I(\vec{x}) & = & [T(\vec{x})T^*(\vec{x})] \otimes \langle \Psi_o(\vec{x};t)\Psi_o^*(\vec{x};t)\rangle & (T(\vec{x}) \text{ is time independent.}) \\
\langle \Psi_o(\vec{x};t)\Psi_o^*(\vec{x};t)\rangle & = & |\Psi_o(\vec{x})|^2 & \text{(complete spatial incoherence)} \\
I(\vec{x}) & = & |\Psi_o(\vec{x})|^2 \otimes [T(\vec{x})T^*(\vec{x})] & \\
I(\vec{x}) & = & I_o(\vec{x}) \otimes [T(\vec{x})T^*(\vec{x})] = I_o(\vec{x}) \otimes P(\vec{x}) & \text{(P: probe intensity)}
\end{array}
$$

Probe function $P(\vec{x})$: source intensity distribution as measured at the sample plane.

Image formation: weak phase approximation

Phase object approximation:

$$\Psi_o(\vec{\rho}) = \exp^{i\sigma V_p(\vec{\rho})}$$

Weak phase object approximation

$$\Psi_o(\vec{\rho}) = 1 + i\sigma V_p(\vec{\rho})$$

Back focal plane:

$$\widetilde{\Psi}_o(\vec{u}) = \delta(\vec{u}) + i\sigma \widetilde{Vp}(\vec{u})$$

Transfer:

$$\widetilde{\Psi}_i(\vec{u}) = \left[\delta(\vec{u}) + i\sigma \widetilde{Vp}(\vec{u})\right] \widetilde{T}(\vec{u})$$

When $\sin\chi(\vec{u}) \approx -1$ (figure):

$$\widetilde{\Psi}_i(\vec{u}) = \delta(\vec{u}) - \sigma \widetilde{Vp}(\vec{u})$$

Image plane:

$$I(\vec{x}) = \Psi_i(\vec{x}) * \Psi_i^*(\vec{x}) \approx 1 + 2\sigma Vp(\vec{x})$$

Atoms are white on a grey background.

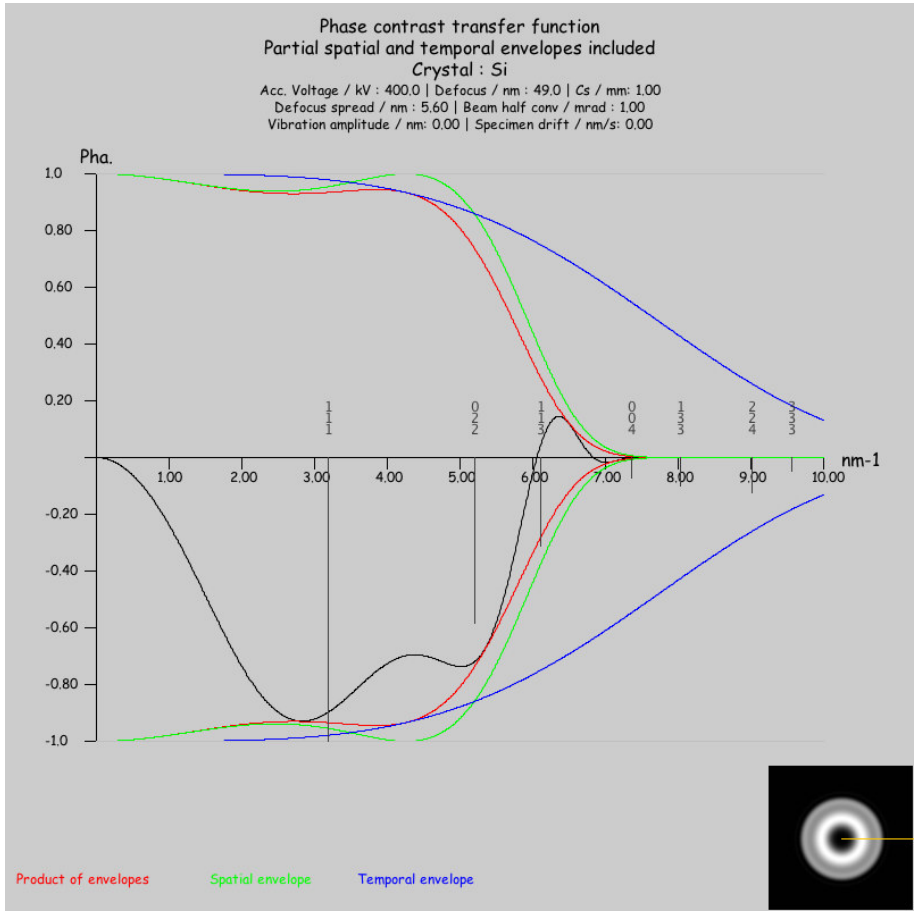

The phase contrast transfer function compensates the phase shift introduced by diffraction.

Image formation: thickness series

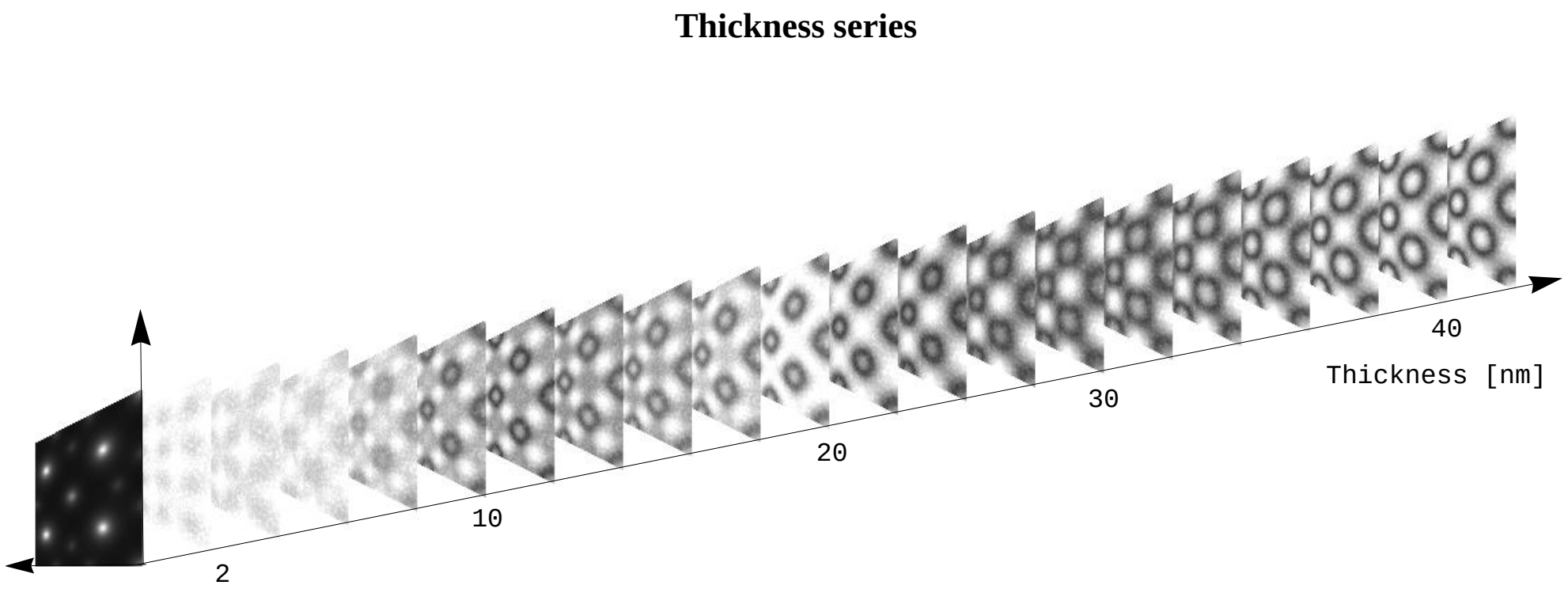

For a very small crystal thickness, a positive Cs objective lens and optimal defocus the atomic columns position appear as black dots in HRTEM (Weak Phase Object Approximation).

Increasing the crystal thickness makes the HRTEM images less straight forward to interpret. In high symmetry zone axis orientation, the electrons channel along the atomic columns and images present contrasts not correlated to them.

HRTEM images map: Si [110], Titan 300 kV, C_s = -33μm

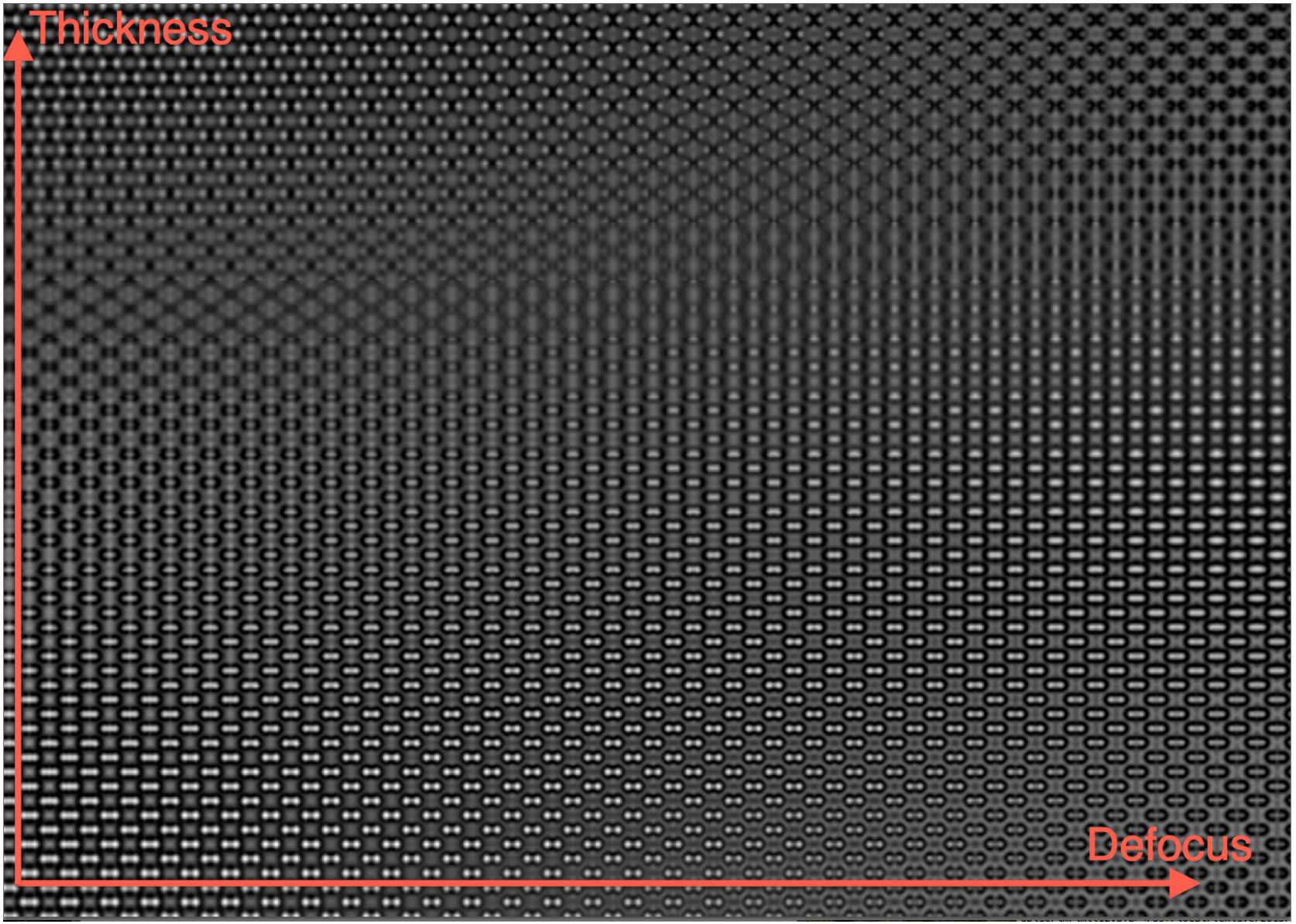

Note that similar images appear at particular thicknesses or defocuses (Fourier images).

STEM probe formation and aberrations

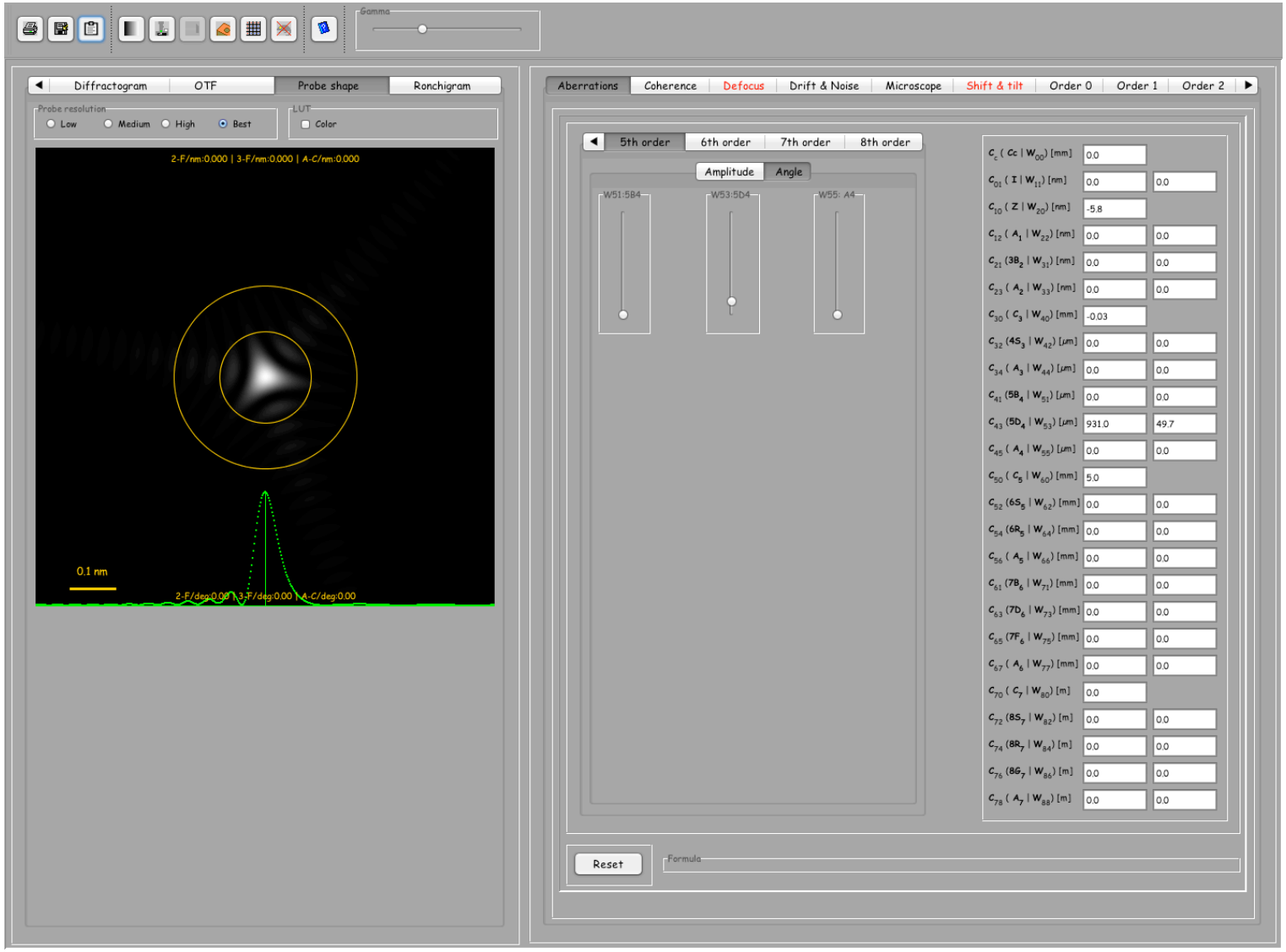

STEM probe with C_{43} geometrical aberration (Krivanek) or W_{53} wavefront aberration or 4th order three-lobe (Haider).

$P(\vec{x})$: source intensity distribution (probe) as measured at the sample plane

2 fold astigmatism.

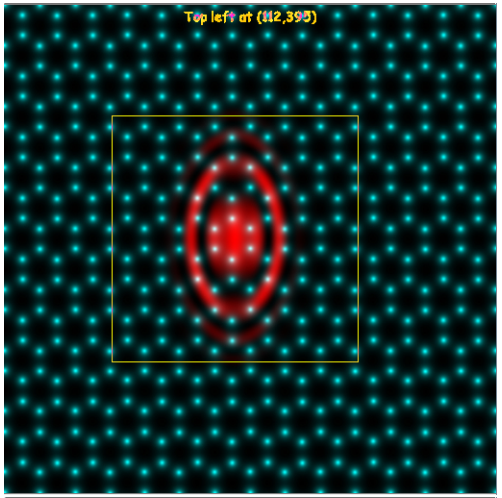

3 fold astigmatism.

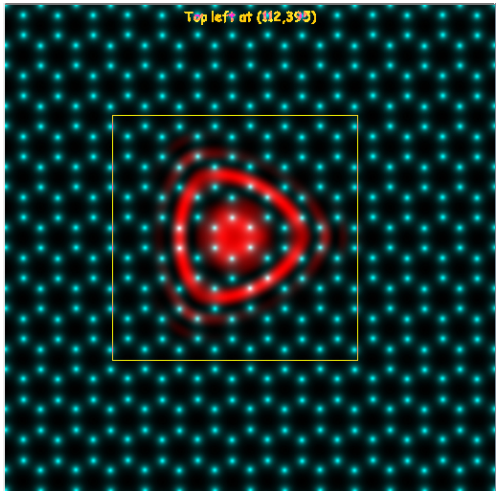

Coma.

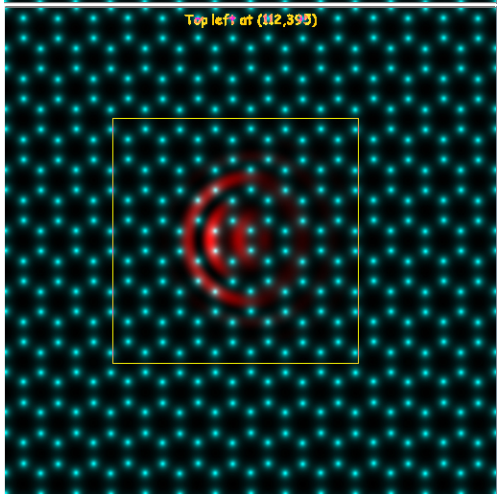

Corrected probe.

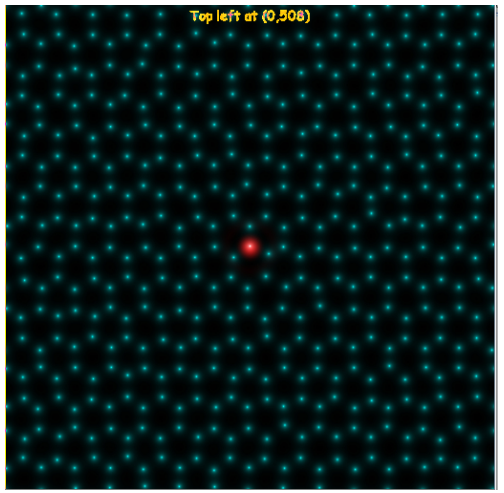

Aberrations modify the source intensity distribution. STEM scans the corrected probe $P(\vec{x})$ on the

STEM imaging: graphene

Proj. pot. approx. Channeling calc.

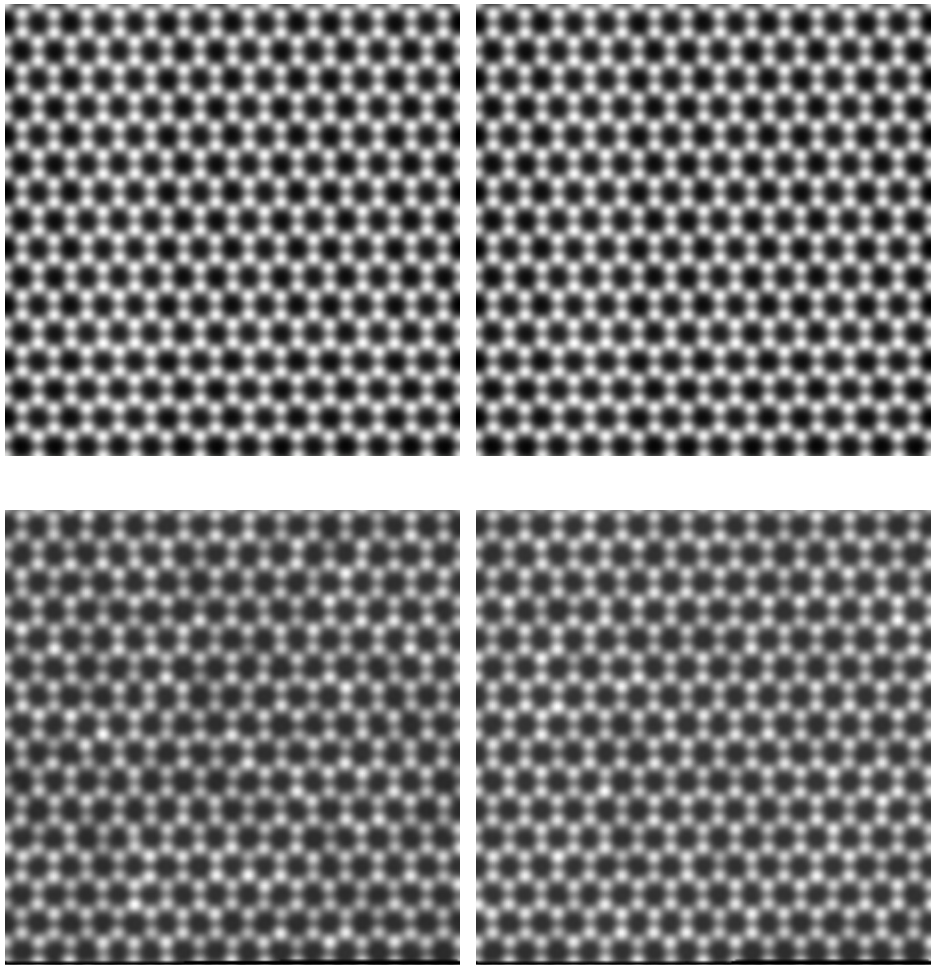

Frozen lattice 5 conf. Frozen lattice 10 conf.

Frozen lattice: sampling is critical and it is necessary to repeat the calculation (10 to 40 times) to image most of the possible atomic configurations.

Detector

HRTEM quantitative match: Stobbs factor?

Do not forget to take into account the MTF of the CCD camera in order to match experimental and calculated images. The transfer of intensity by the CCD camera is described by its **Modulation Transfer Function**.

Detectors: CCD cameras

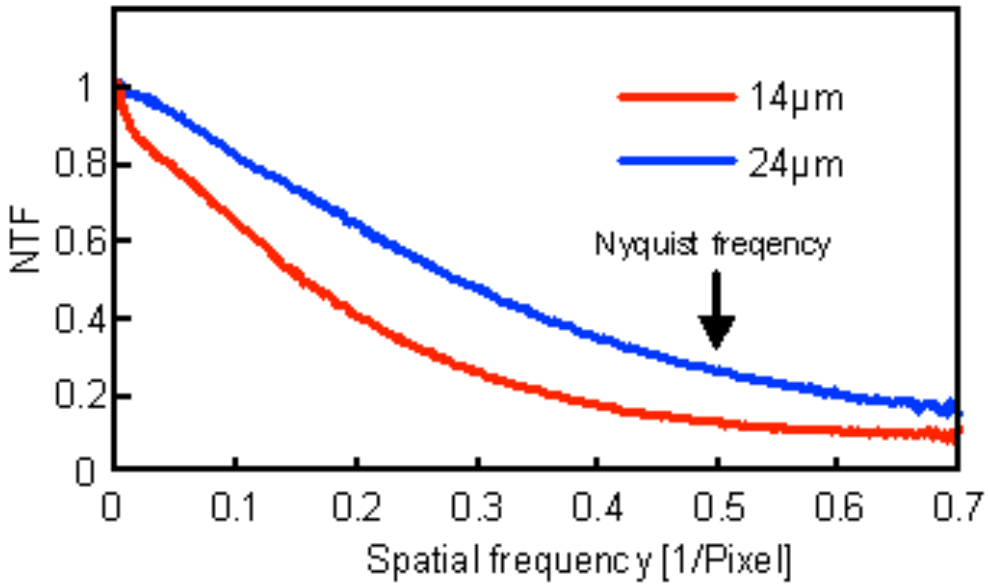

Noise tranfer function (NTF) of 2k cameras with 14 µm and 24 µm pixel size (corrected for aliasing)

Comparison of the MTF of 2 CCD cameras. Note that the intensity of high spatial frequencies is severely attenuated.

Given a particular crystal, the contrast of the observed HRTEM micrographs depends on the TEM magnification. For quantitative work always record HRTEM micrographs at the highest possible magnification or introduce the detector MTF in the simulations.

MTF & Si (220) lattice planes

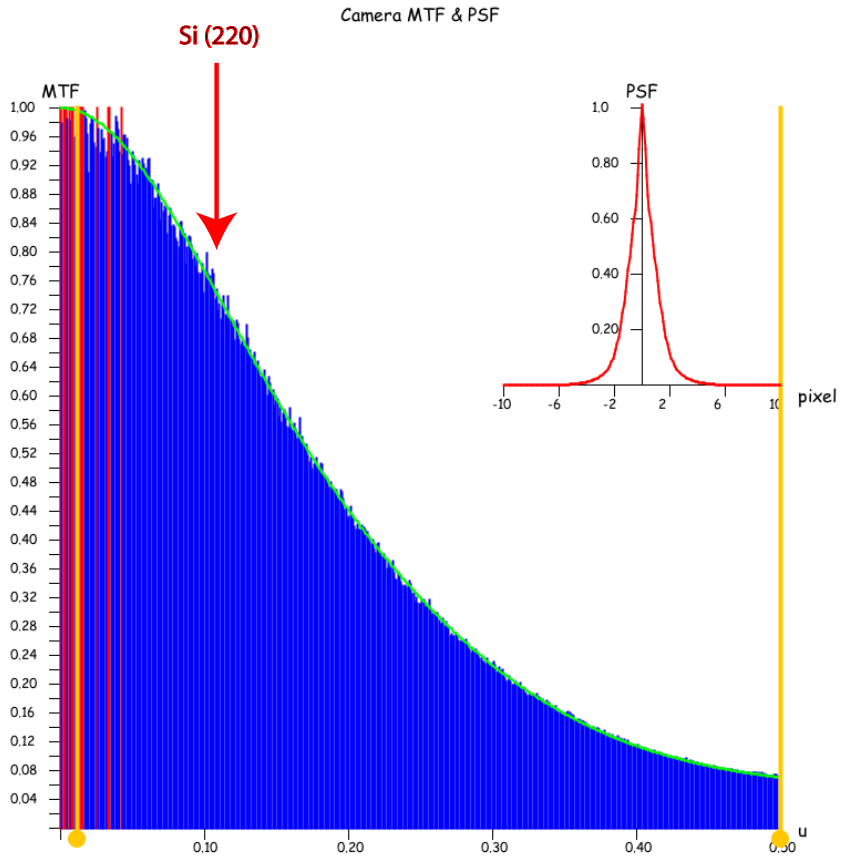

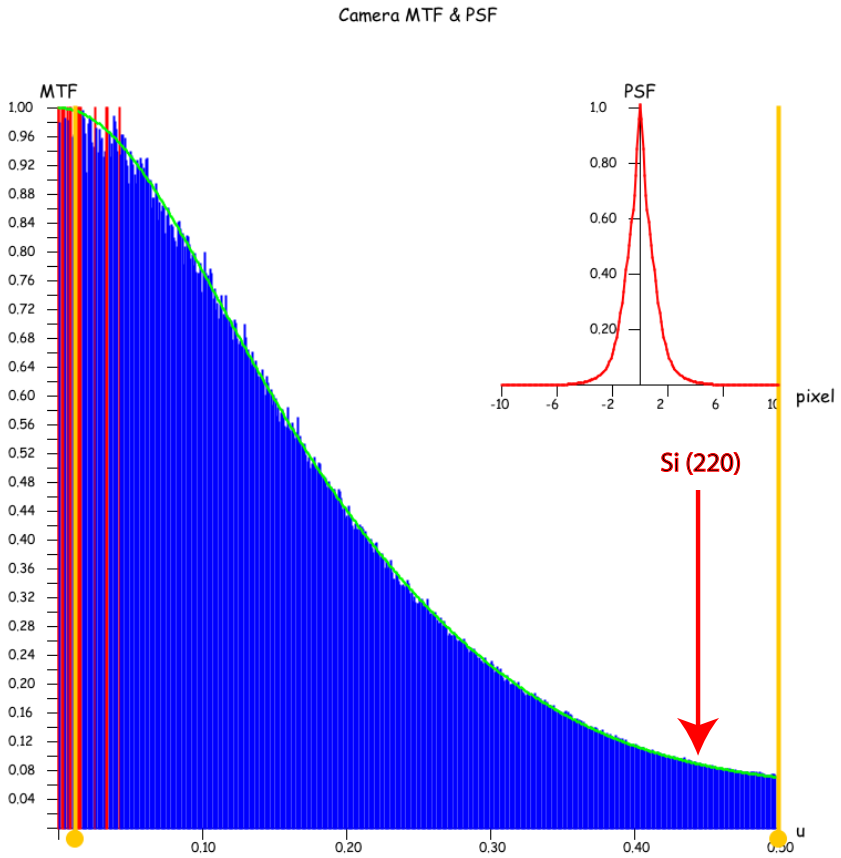

Si (220) spatial frequencies at low and high magnification (i.e. diffracted beams).

Effect of CCD MTF on simulated images: high magnification

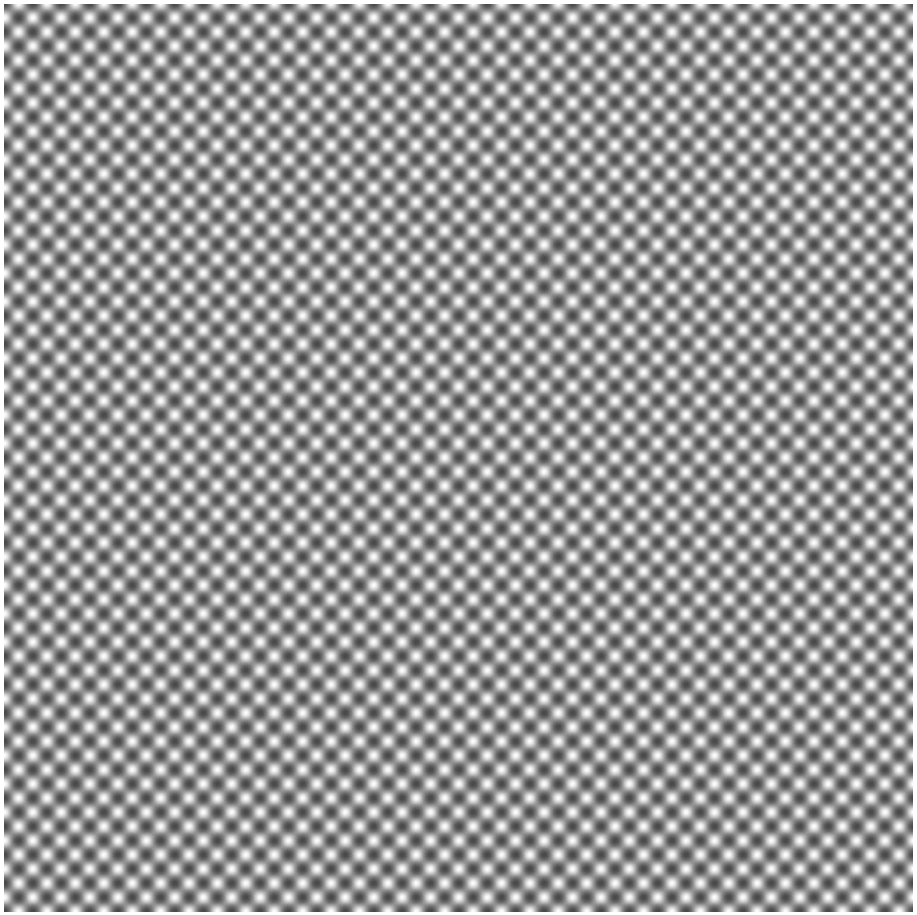

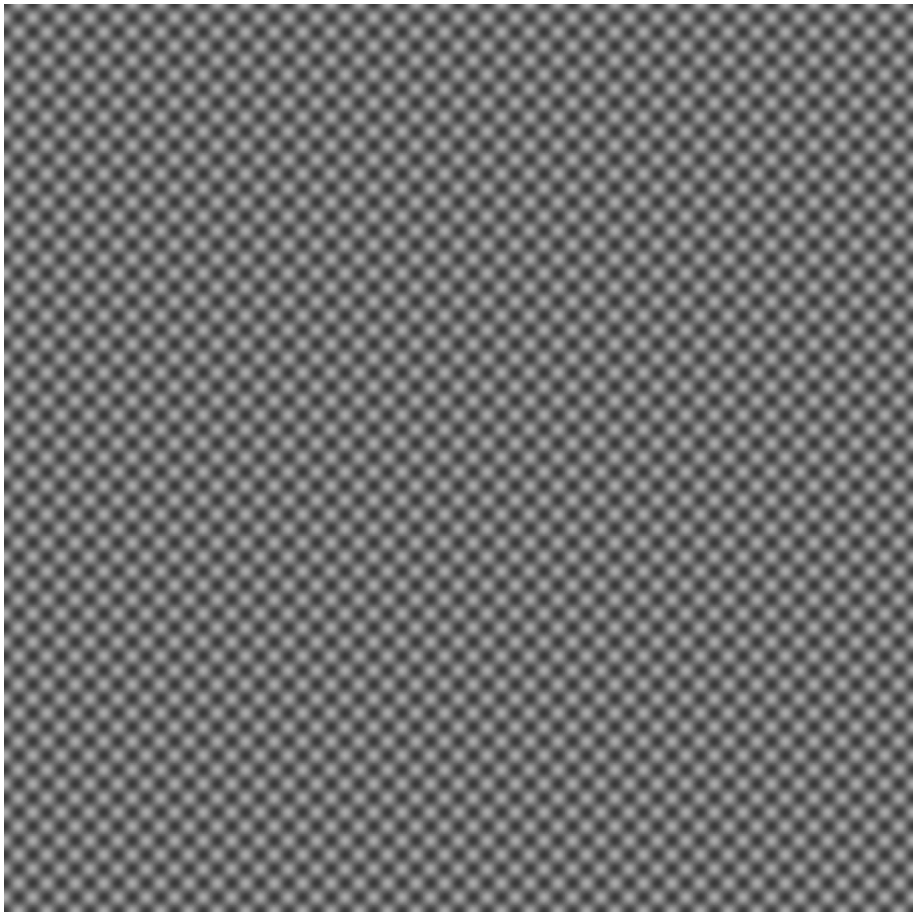

Taking into account the MTF of the CCD camera (left: CCD MTF not included, right: CCD MTF included).

Effect of CCD MTF on simulated images: low magnification

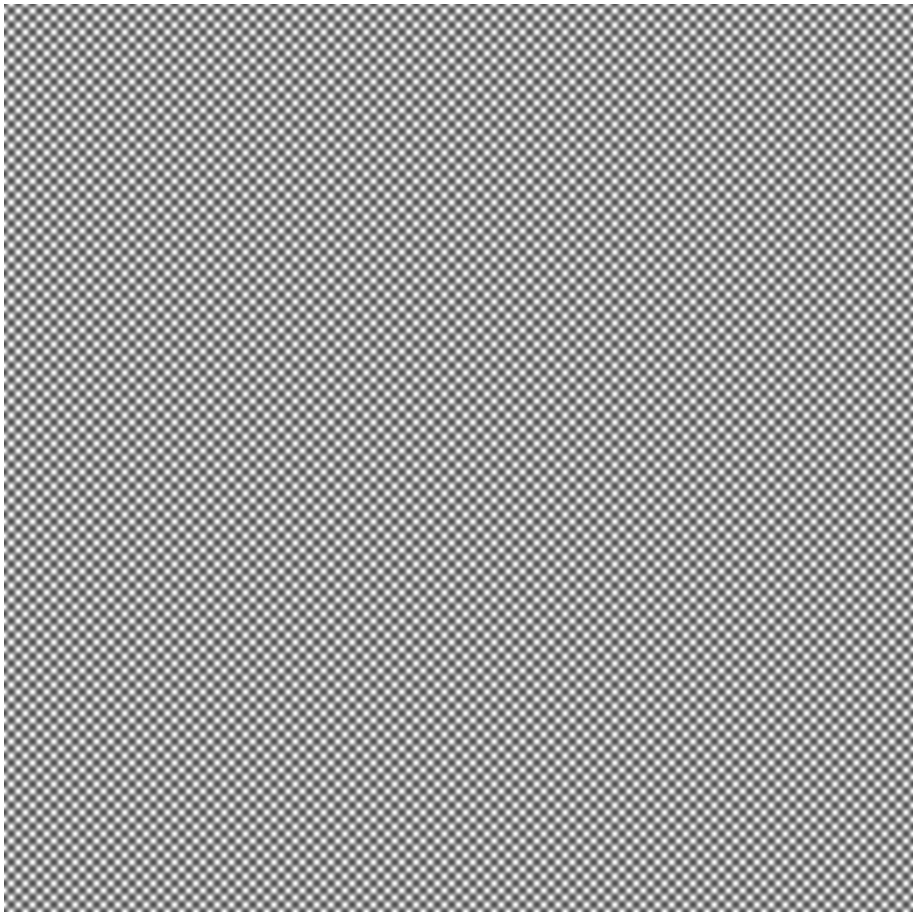

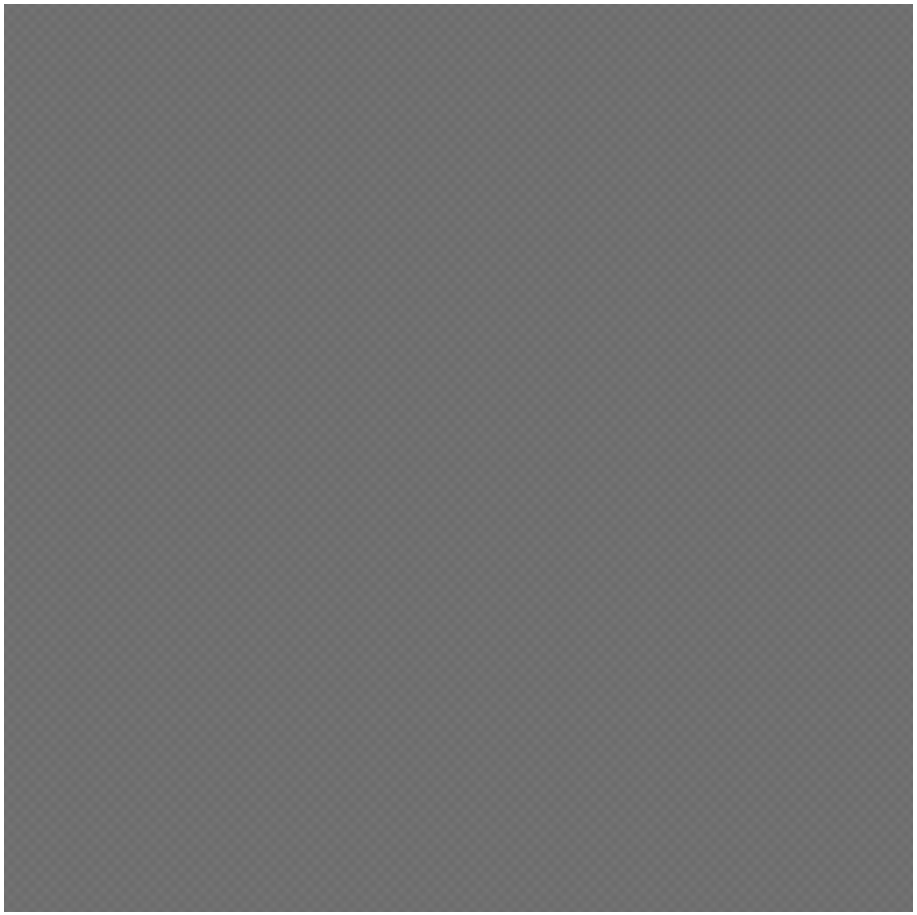

Taking into account the MTF of the CCD camera (left: CCD MTF not included, right: CCD MTF included).

How to understand HRTEM image formation?

Read books, research and review papers and... use an image simulation program

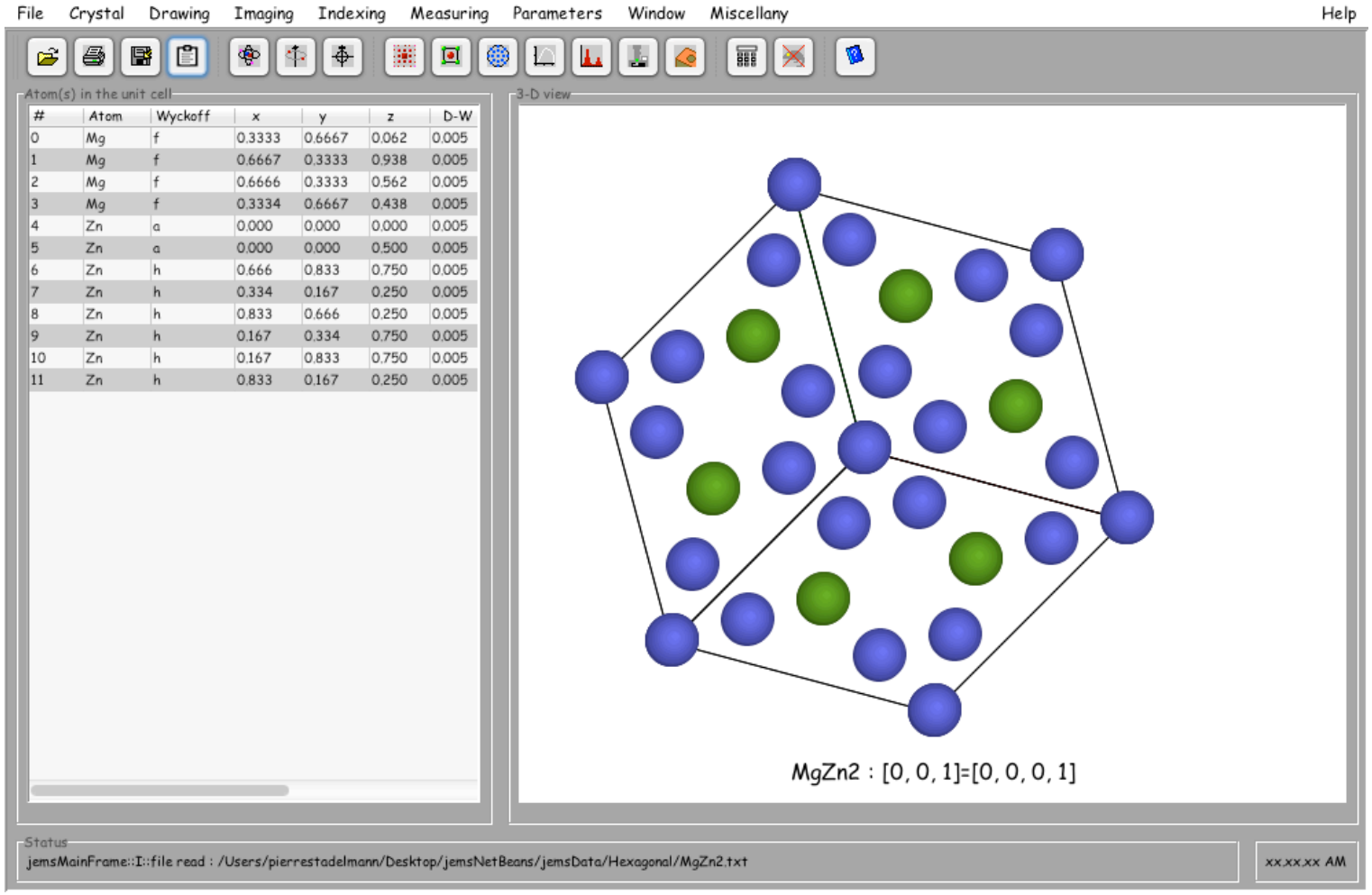

jems allows to perform many kind of image simulations. The student edition is freely downloadable [a] and ready for Mac OS 10, Windows 7, 8 or 10 and Linux ubuntu 64 bits.

[a] http://www.jems-saas.ch/

Image simulation labs

Have jems installed on your PC or Mac before the labs. (I can also provide jems on USB keys in case you can't download it.) You will have to request a license code (see installation instructions). The license code will be valid to June 30 2020.

`http://www.jems-saas.ch/`
`http://www.jems-saas.ch/home/jemsv4_7428u2019.htm`

3 versions are available for download:

1. MacOS-X 10.7 to 10.14 (Mojave)
2. Windows 7 to 10.
3. Linux ubuntu 15.04 or later.